Plant Cell Tiss Organ Cult (2017) 129:411–430
DOI 10.1007/s11240-017-1188-5

ORIGINAL ARTICLE

GsJ11, identified by genome-wide analysis, facilitates alkaline tolerance in transgenic plants

Xuewei Song[1] · Huizi Duanmu[1] · Yang Yu[1] · Chao Chen[1] · Xiaoli Sun[2] · Pinghui Zhu[1] · Ranran Chen[1] · Xiangbo Duan[1] · Huiqing Li[1] · Lei Cao[1] · Zaib un Nisa[1] · Qiang Li[1] · Yanming Zhu[1] · Xiaodong Ding[1]

Received: 13 September 2016 / Accepted: 7 February 2017 / Published online: 11 March 2017

Abstract DnaJ/Hsp40, one of molecular chaperones heat shock proteins (Hsps), is a kind of key components to contribute in cellular homeostasis under adverse growth conditions. However, until now, only few researches focus on its functions under alkaline stress response which tremendously inhibit plant growth and development, especially the DnaJ genes from wild soybean. In this study, we identified and characterized 196 DnaJ genes in soybean genome. We determined sequence information, conserve domains, gene structure, evolutionary relationship and chromosomal location of all the family members. Then, we investigated the expression profiles of DnaJ family genes in wild soybean under alkaline stress. According to heat map and our previous RNA-seq data, *GsJ11*, significantly induced by $NaHCO_3$ treatment, was further selected. Moreover, we determined the temporal and spatial expression patterns of *GsJ11* in wild soybean and characterized its physiological functions by using transgenic *Arabidopsis* and *atj11* mutant *Arabidopsis*. Our results suggest that *GsJ11* was moderately expressed in roots of wild soybean and could highly be induced by $NaHCO_3$ in 3 h, and its *Arabidopsis* overexpression lines exhibited higher but the *atj11* mutant lines showed lower tolerance to $NaHCO_3$ than the WT line. Furthermore, we found that the transcript levels of stress-inducible genes were up-regulated in *GsJ11* overexpression lines. Taken together, our results demonstrate that *GsJ11* acts as a positive regulator in plant responses to bicarbonate alkaline stress.

Keywords Molecular chaperones · DnaJ · *Glycine soja* · *Arabidopsis* · Alkaline stress

Introduction

Plants have evolved adaptive mechanisms to defense adverse environments as they are nonmotile, including regulating the specific genes' expression and producing a large number of stress-related proteins to response various stress (Zhai et al. 2016). DnaJs/Hsp40s (heat-shock protein 40) is a large ubiquitous family which functions in a myriad of cellular processes as a co-chaperone component for Hsp70s machinery (Kampinga and Craig 2010; Qiu et al. 2006; Silver and Way 1993; Vitha et al. 2003). DnaJ proteins contain a highly conserved 70-amino-acid consensus sequence known as J domain, and they can bind and regulate Hsp70 proteins by J domain (Hennessy et al. 2005; Jiang et al. 2007). DnaJ has conservatism throughout evolutionary process and facilitates the protein folding and refolding, and also play important roles for protein translation, translocation, and degradation (Chen et al. 2010; Wang et al. 2004). Expression of heat-shock proteins *in planta* can be induced by a variety of environmental stresses, such as soil salinity, high temperature, cold, osmotic and oxidative stresses (Dekker et al. 2015). For example, *BIL2*, encoding mitochondria-localized heat shock protein, enhanced resistance

Electronic supplementary material The online version of this article (doi:10.1007/s11240-017-1188-5) contains supplementary material, which is available to authorized users.

✉ Yanming Zhu
ymzhu2001@neau.edu.cn

✉ Xiaodong Ding
Xiaodong.ding@neau.edu.cn

[1] Key Laboratory of Agricultural Biological Functional Genes, Northeast Agricultural University, Harbin, People's Republic of China

[2] Agronomy College, Heilongjiang Bayi Agricultural University, Daqing, People's Republic of China

against salt and high light stress in brassinosteroid signaling if overexpressed in *Arabidopsis* (Bekh-Ochir et al. 2013). *AtDjA3* gene is expressed in various tissues, and its expression could be induced by heat, cold, drought, osmotic shock stresses and ABA (Salas-Munoz et al. 2016), and also under saline conditions with alkaline pH (Yang et al. 2010). Therefore, DnaJ proteins are widely considered as cellular stress adapter (Piippo et al. 2006; Rajan and D'Silva 2009; Scarpeci et al. 2008).

Alkaline soils are widely spread in the world and severely affect the terrestrial ecology, and subsequently limit agricultural productivity globally. Previously reports have clearly defined salt stress and alkaline stress, salt stress is mainly caused by neutral salts such as NaCl and/or Na_2SO_4, while alkaline stress is mainly caused by alkaline salts like $NaHCO_3$ and/or Na_2CO_3 (Shi and Wang 2005). Salt stress in soil generally involves osmotic stress and ion-induced injuries (Munns 2002); there are similar problems for alkaline stress but with additional high-pH influence. Alkaline stress can severely affect soil structure, interfere with essential micro nutrients uptake and upset intracellular ion balance in plant (Yang et al. 2007). Plant grown in alkaline soil showed reduced leaf area, leaf length and leaf width, consequently organism shoot biomass is decreased. The diminished leaf area is mainly contributed to decreased photosynthetic rate and stomatal conductance in alkaline-induced leaf chlorosis (Bie et al. 2004). Alkaline environment surrounding the root can inhibit root respiration and affect accumulation and compartmentation of organic acids in root cells (Lee and Woolhouse 1969; Yang et al. 1994). It can also lead metal ions and phosphorus to precipitate, with loss of the normal physiological functions of root and destruction of the root cell structure (Li et al. 2009). Those inhibitory effects would cause reduced root growth and elongation. Plants exposed to $NaHCO_3$ produced more reactive oxygen species (ROS, O_2^-, H_2O_2), and exhibited increased activities of antioxidant enzymes (SOD, POX) at a low concentration of $NaHCO_3$ (Gong et al. 2014; Guan et al. 2016).

In previous reports, PROTEIN KINASE5 (PKS5) and the chaperone DNAJ HOMOLOG3 (J3) in *Arabidopsis thaliana* are responsive to salt at alkaline pH via regulating the interaction between PM H^+-ATPase and 14-3-3 proteins (Fuglsang et al. 2007; Yang et al. 2010). Similar, 14-3-3 protein TFT4 regulates PKS5-J3 signaling pathway and significantly enhanced H^+ efflux and the activity of PM H^+-ATPase in the root tips and increased plant alkaline resistance in tomato (Xu et al. 2013). As wild soybean (*Glycine soja*) G07256 is an ideal candidate for exploring resistant genes and breeding of transgenic legume crops with superior salt-alkaline tolerance (Chen et al. 2013). We have identified and characterized a couple of genes including a chaperone 14-3-3 gene from wild soybean (Liu et al. 2015; Sun et al. 2015, 2016; Yu et al. 2016). These genes are initially identified from a transcriptome analysis of *G. soja* roots under $NaHCO_3$ stress on the Illumina Genome Analyzer IIx (GAIIx) platform (DuanMu et al. 2015).

Here we systematically compared the evolutions and diversities of DnaJ family genes and investigated their expression profiles in wild soybean based on the transcriptome data of *G. soja* under $NaHCO_3$ stress, and identified one DnaJ gene, *GsJ11*, which was significantly responsive to $NaHCO_3$ treatment. Moreover, we found the gain-of-function of *GsJ11* and loss-of-function mutants of its homologous gene in *Arabidopsis* significantly altered plant alkaline resistance and physiological indices, providing the clues to understand the novel functions of DnaJ proteins and the mechanism of plant alkaline resistance.

Materials and methods

Database searches, identification and gene classification of DnaJ family genes in soybean

Previously identified ten different species and three types of DnaJ protein sequences were used as queries to establish a Hidden Markov model. Although the genome of wild soybean (*Glycine soja*) was sequenced, the well-annotated database is still not available (Qi et al. 2014). Since the cultivated soybean (*Glycine max*) is the close relative of *G. soja*, here, we searched for DnaJ members by using soybean (Glycine max Wm82.a2.v1) database with the HMM file. All information about soybean DnaJ genes, including sequences ID, gene locations on chromosomes, sequences lengths of DNA, cDNA, coding sequence (CDS) and protein were obtained from Phytozome (https://phytozome.jgi.doe.gov/pz/portal.html). ExPASy online software (http://web.expasy.org/protparam/) was used to calculate physical parameters such as the molecular mass (kD), and isoelectric point (pI) of all the predicted DnaJ proteins (Feng et al. 2015). Positions of J domain were obtained from NCBI Conserved Domain Search program (http://www.ncbi.nlm.nih.gov/Structure/cdd/wrpsb.cgi). All potential candidate proteins were analyzed to verify the presence of the J domain using SMART (Simple Modular Architecture Research Tool) tools (http://smart.embl-heidelberg.de/) (Letunic et al. 2015) and Pfam (http://pfam.sanger.ac.uk/) database. In addition, SMART tool was also subjected to analysis of the obtained sequences structures (Schultz et al. 2000).

Multiple alignment and phylogenetic analysis

Multiple sequence alignment of all the members of DnaJ family protein was performed using ClustalX 2.0 software

with default parameters (Larkin et al. 2007). Based on the alignment, the phylogenetic tree was constructed with MEGA 5.0 software, by using the maximum likelihood (ML) method and 500 replications for the 500 bootstrap resampling (Li et al. 2015).

Exon/intron organization, chromosomal location and gene duplication

A schematic diagram of the gene Exon/intron organization of DnaJ genes was executed through the Gene Structure Display Server (GSDS: http://gsds.cbi.pku.edu.cn/) (Hu et al. 2015). Based on the position information obtained from Phytozome database (http://www.phytozome.net), the chromosomal location image of the DnaJ family genes was generated by using the MapInspect software (http://www.plantbreeding.wur.nl/uk/software_mapinspect.html) (Wu et al. 2015).

Microarray analysis

The microarray data for gene expression in root and leaf of wild soybean (*G. soja*) under alkaline stress was downloaded from the NCBI Gene Expression Omnibus (http://www.ncbi.nlm.nih.gov/geo/) database under accession numbers GSE17883 and GSE20323. By comparing the variation of gene expression levels between treated and control samples, differential expression genes were selected ($|\log_2 \text{Ratio}|>1, p<0.05$) and a heat map was generated using the MATLAB software.

Plant materials, growth conditions, and stress treatments

To illustrate the expression patterns of the target gene under bicarbonate treatment, the seeds of wild soybean (*G. soja* 07256) line were obtained from the Jilin Academy of Sciences (Changchun, China). For the purpose of surface sterilization, the *G. soja* seeds were firstly shaken for 15 min in 98% sulfuric acid and then washed by sterilized distilled water for 3 times, and followed by incubation in dark for 24 h to break seeds dormancy. The geminating seeds were grown in 1/4 Hoagland solution at 24–28 °C and 16 h light/8 h dark cycles for 3 weeks. The nutrient solution should change every 3 days. 21-day-old seedlings were transferred into 1/4 Hoagland solution with 50 mM $NaHCO_3$. The root samples were collected at six independent time points (0, 1, 3, 6, 12 and 24 h) and were stored in liquid nitrogen.

Columbia ecotype (Col-0) strain of *Arabidopsis thaliana* was used in this study as wild type plant, and also used for generating overexpressing lines. T-DNA insertion mutant line of *atj11* (SALK_015630 C) were obtained from The Arabidopsis Information Resource center (TAIR) and identified by PCR and semi-quantitative RT-PCR. The gene specific primer pairs were used for PCR: LP 5′-TTATGG CTGCATCCCTAATTG-3′ and RP 5′-TTCTTCTCCGCC TCTATCTCC-3′ and left border T-DNA primer LBb1.3 5′-ATTTTGCCGATTTCGGAAC-3′. The specific primers used for semi-quantitative RT-PCR were as follows: 5′-GAAGATCCATGCCGCTTACTG-3′ and 5′-CGGAGG AAACACAGAATACCC-3′.

For surface sterilization, the seeds of *Arabidopsis* were shaken for 6 min in 5% NaClO and then washed with distilled water for 6 times to remove residues completely. After that, the sterilized seeds were incubated at 4 °C for 3 days to break dormancy, and then the seeds were sown on 1/2 MS solid medium under controlled environmental condition (21–23 °C, 100 μmol photons m^{-2} s^{-1}, 60% relative humidity, 16 h light/8 h dark cycles). To analyze the expression of stress-responsive marker genes, 14-days-old seedlings of WT, *GsJ11* OX and *atj11* lines were treated with water or 50 mM $NaHCO_3$ solution and then were sampled at various time points (0, 3, 6 and 12 h) from 3 biological replicates after treatments.

Quantitative real-time PCR

Total RNA was extracted as per described by EasyPure Plant RNA Kit protocol (Transgen Biotech, China) from *G. soja* or *Arabidopsis* seedlings. RNA samples were used for reverse transcription with SuperScriptTM III Reverse Transcriptase kit (Invitrogen, Carlsbad, CA, USA). Quantitative real-time PCR was performed using SYBR Green Master Mix (TaKaRa, Shiga, Japan) to detect transcript levels. *GADPH* (*Glycine soja*) and *ACTIN2* (*Arabidopsis thaliana*) were used as internal references. All experiments were carried out with three independent biological replicates for statistical analyses. The relative expression levels were calculated by using $2^{-\Delta\Delta CT}$ method (Steibel et al. 2005). The gene specific primers used for quantitative real-time PCR were listed in Online Resource 1.

Vector construction and generation of transgenic *Arabidopsis thaliana*

The full-length *GsJ11* coding DNA sequence was cloned by USER cloning method with primer pairs: 5′-GGCTTA AUATGATTTCTTCCGTGTCC-3′ and 5′-GGTTTAAUC TACCAGCACTGATCCGT-3′ (Nour-Eldin et al. 2006). The PCR products were inserted into pCAMBIA330035Su USER vector and sent for sequencing. The recombinant vector pCAMBIA330035Su-GsJ11 was transformed in to *Agrobaterium tumefaciens* strain LBA4404 and transformed into wild-type *Arabidopsis* by floral dip method. The T_0 generation seeds were germinated and selected on

1/2 MS medium supplemented with 50 mg/L phosphinothricin ammonium. The transformants were selected and identified by PCR with the above gene cloning primers. Homozygous OX lines were selected by genotyping of T_2 generations on screening medium and identified by PCR with gene specific primers and semi-quantitave RT-PCR with primer pairs: 5′-ATGATTTCTTCCGTGTCCTTTCC-3′ and 5′-CTACCAGCACTGATCCGTTTCC-3′.

Phenotypic analysis of *Arabidopsis* plants

For germination analysis, the seeds of *GsJ11* OX, WT and mutant lines were germinated on 1/2 solid medium supplemented with 0, 6, 7 or 8 mM $NaHCO_3$. The germination profiles were recorded according to emergence of seed radicals for consecutive 7 days after sowing, and photos were taken to display the growth performance of each line. For each experiment, 120 seeds were used in total and experiments were repeated at least in three times.

To investigate the stress resistance at seedling stage, 7-days-old seedlings of *GsJ11* OX, WT and mutant lines were grown on normal 1/2 MS solid medium and then transferred to medium supplemented 6 or 7 mM $NaHCO_3$ for 6 days. After that, we measured and recorded the primary root length of every seedling for statistics analysis. For each experiment, 15 seedlings were used in total and all experiments were also repeated at least three times.

To characterize the phenotype at adult stage, the seeds of each line were sown in the mixture of garden soil: peat moss: vermiculite (volume ratio, 1:1:1). 4-week-old plants were irrigated with150 mM $NaHCO_3$ after every 3 days for a total of 14 days. The photographs were taken before and after 14-day treatment.

Statistical analysis

Each group experiments were repeated at least three times. Data were expressed as mean ± SD. Data were analyzed statistically using Duncan's multiple range tests or Student's *t* test. Results were considered statistically significant different when $P < 0.05$.

Results

Identification and classification of DnaJ family genes

DnaJ proteins are important components for protein translation, folding, unfolding, translocation, and degradation in cells (Yang et al. 2010). In this case, we aimed to identify all DnaJ family members from soybean genome. Totally 214 non-redundant DnaJ genes were identified by using the soybean database. All the obtained protein sequences were subjected to SMART and Pfam online tools to ensure that the potential candidates contain J-domain; those lacking the conserved domain were ignored. Finally, we obtained 196 DnaJ family members, and the detailed information of them was exhibited in Table 1. Interestingly, dissimilar to other Hsp protein families, the average molecular mass and isoelectric point of J-proteins are significantly large. The polypeptides range from 68 to 2589 amino acids long, with calculated molecular mass between 7.72 and 283.51 and isoelectric point values of 4.21–11.09.

For a better understanding of DnaJ family in soybean, we performed structural classification of J proteins. As shown in Online Resource 2, the DnaJ proteins could be clustered into three types (I, II and III). Type I J proteins, as the typical DnaJ molecular chaperone model, contain four domains, an N-terminal J-domain was connected with a glycine-rich domain (G/F domain), and followed by a zinc-finger domain and a distal carboxy-terminal (C-terminal) domain, whereas type II J proteins lack the zinc-finger domain. Type III J proteins only have a J domain but lack the other sequence features that are found in type I and II members of the family.

Multiple sequence alignments and phylogenetic analyses of DnaJ family

To further clarify the characteristics of the conserved domain architectures, we aligned all soybean J proteins by ClustalX2.0 (Fig. 1). Coinciding with the classification results above, the 196 DanJ proteins were able to be clustered into three groups with 20 type I, 23 type II and 153 type III, respectively. All type I J-proteins possess 4 characteristic domains including a compact helical J domain, a proximal G/F domain which is rich in Gly/Phe, a $(CXXCXGXG)_4$ zinc-finger domain and a less conserved carboxy-terminal (Fig. 1a). Type II J proteins are similar to type I except they do not have zinc-finger domain (Fig. 1b) and type III just have J-domain (Fig. 1c). Furthermore, we found a highly conserved tri-peptide composed of His, Pro and Asp (HPD motif) in all of J domains which may be crucial for functions of J-proteins.

To further clarify the complexity of DnaJ proteins in soybean, we then explored the evolutionary relationships among DnaJ proteins of soybean. A phylogenetic tree was constructed by maximum likelihood (ML) method with 500 bootstrap replicates using all the full-length J-proteins from soybean (Fig. 2). The data showed that these DnaJ sequences fall into three clusters, consistent with above the sequence alignment results. This work provides a considerable basis for structural and functional characterization of soybean J proteins.

Table 1 The detailed information of DnaJ gene family members in soybean

Sequenced ID	Location	Sequence length			Protein			Position of J domain
		DNA (bp)	mRNA (bp)	CDS (bp)	Length (a.a.)	Mol.wt.(kD)	PI	
Glyma.01G013800	Chr01:1314163..1316550	2388	2388	1686	561	63.28	9.31	59–120
Glyma.01G023800	Chr01:2426625..2433075	6451	1458	1458	485	54.35	9.75	55–119
Glyma.01G036500	Chr01:3821377..3825854	4478	2011	1233	410	46.26	8.97	22–84
Glyma.01G040600	Chr01:4389420..4392033	2614	1440	834	277	31.49	8.67	5–71
Glyma.01G121300	Chr01:41795455..41800252	4798	1618	1014	337	37.19	9.66	4–67
Glyma.01G166000	Chr01:50355756..50357120	1365	1365	477	158	17.47	9.94	64–128
Glyma.01G191500	Chr01:52609450..52614224	4775	1977	1626	541	61.9	7.32	67–131
Glyma.01G209800	Chr01:54132733..54141714	8982	2244	1623	540	59.95	9.49	12–77
Glyma.01G227100	Chr01:55558004..55563706	5703	2895	2319	772	86.16	6.25	655–737
Glyma.01G245700	Chr01:56815824..56824795	8972	957	732	243	27.11	5.18	6–68
Glyma.02G013800	Chr02:1246969..1251772	4804	1568	1041	346	39.13	5.68	26–88
Glyma.02G023500	Chr02:2120957..2123333	2377	1475	831	276	31.57	8.83	5–71
Glyma.02G029600	Chr02:2718387..2723154	4768	2023	1242	413	46.69	8.80	25–87
Glyma.02G047900	Chr02:4402299..4403204	906	906	309	102	11.65	9.78	6–70
Glyma.02G172700	Chr02:27419070..27424482	5413	1297	726	241	28.17	9.72	183–237
Glyma.02G179900	Chr02:30631549..30634896	3348	1455	843	280	32.2	8.27	28–90
Glyma.02G211200	Chr02:39637739..39651535	13,797	1683	1410	469	52.59	8.89	83–145
Glyma.02G212500	Chr02:39851468..39854914	3447	931	468	155	18.3	8.90	57–119
Glyma.02G213900	Chr02:40001858..40004507	2650	2650	1047	348	38.17	8.38	67–129
Glyma.02G305000	Chr02:47994943..47998270	3328	2899	2118	705	78.14	8.27	66–127
Glyma.03G057500	Chr03:8117254..8122189	4936	1471	1014	337	37.16	9.65	4–67
Glyma.03G116600	Chr03:32527885..32532444	4560	1885	1263	420	47.16	7.09	15–72
Glyma.03G133500	Chr03:34865704..34878669	12,966	4813	3867	1288	139.57	7.51	1135–1218
Glyma.03G144900	Chr03:36047632..36050893	3262	546	213	70	7.53	6.7	12–65
Glyma.03G179800	Chr03:39203079..39208383	5305	2005	1473	490	54.25	5.78	373–436
Glyma.03G216900	Chr03:42087292..42089007	1716	892	462	153	17.53	6.52	12–78
Glyma.03G218300	Chr03:42186854..42191345	4492	1749	1032	343	38.81	6.72	26–88
Glyma.03G218600	Chr03:42212143..42215618	3476	2390	1713	570	63.51	9.06	401–435
Glyma.03G223300	Chr03:42601145..42604438	3294	986	408	135	14.88	10.15	9–62
Glyma.03G232700	Chr03:43368822..43370172	1351	993	492	163	18.42	5.74	12–78
Glyma.03G237900	Chr03:43760175..43762792	2618	1317	756	251	27.76	7.02	50–105
Glyma.03G242300	Chr03:44030745..44036313	5569	4364	3204	1067	119.52	9.25	67–128
Glyma.04G048400	Chr04:3897082..3905394	8313	1362	681	226	27.06	9.88	161–215
Glyma.04G072000	Chr04:6005854..6007339	1486	780	780	259	28.75	8.40	4–59
Glyma.04G094000	Chr04:8359193..8360588	1396	1396	741	246	27.05	5.12	67–129
Glyma.04G148200	Chr04:30302700..30304487	1788	1597	1098	365	40.99	8.19	116–169
Glyma.04G175100	Chr04:43754084..43760083	6000	1949	1056	351	38.92	9.46	4–59
Glyma.04G196300	Chr04:46817780..46822160	4381	3075	2442	813	91.79	8.67	66–119
Glyma.04G237600	Chr04:50613749..50619304	5556	3159	2079	692	79.13	8.78	67–128
Glyma.04G254700	Chr04:52128959..52131698	2740	747	747	248	29.2	9.41	55–123
Glyma.05G012400	Chr05:1151734..1171083	19,350	8504	7770	2589	283.51	5.73	1543–1584
Glyma.05G021300	Chr05:1882386..1885780	3395	2259	1863	620	70.95	5.30	10–76
Glyma.05G083800	Chr05:14017419..14020867	3449	932	339	112	12.03	11.09	29–103
Glyma.05G099600	Chr05:26402103..26402462	360	333	333	110	13.08	9.13	2–50
Glyma.05G119200	Chr05:31210649..31211501	853	853	567	188	21.55	10.29	52–118
Glyma.05G152800	Chr05:34653707..34656176	2470	767	555	184	21.34	10.25	49–113
Glyma.05G177100	Chr05:36577541..36583451	5911	2175	1302	433	46.87	9.66	78–139
Glyma.06G049600	Chr06:3736910..3742779	5870	1836	666	221	26.54	9.97	156–217
Glyma.06G073300	Chr06:5651331..5654202	2872	1745	981	326	35.9	8.38	4–67
Glyma.06G107400	Chr06:8635601..8638796	3196	1399	807	268	31.7	10.34	75–143
Glyma.06G126400	Chr06:10356650..10362151	5502	3186	2079	692	78.85	8.17	67–128
Glyma.06G149700	Chr06:12229701..12233916	4216	612	612	203	22.95	6.23	134–198
Glyma.06G169500	Chr06:14152799..14157127	4329	2994	2382	793	89.21	8.74	66–127

Table 1 (continued)

Sequenced ID	Location	Sequence length			Protein			Position of J domain
		DNA (bp)	mRNA (bp)	CDS (bp)	Length (a.a.)	Mol.wt.(kD)	PI	
Glyma.06G189700	Chr06:16634348..16639910	5563	1958	1056	351	38.7	9.45	4–67
Glyma.06G217000	Chr06:22812652..22815136	2485	2293	1095	364	40.73	7.89	116–177
Glyma.06G275400	Chr06:46631440..46637225	5786	1472	999	332	37.32	7.29	67–129
Glyma.06G289000	Chr06:47766806..47769861	3056	1487	1059	352	38.46	9.59	4–67
Glyma.07G021800	Chr07:1697119..1698666	1548	1173	471	156	17.62	5.72	45–96
Glyma.07G043100	Chr07:3578852..3583051	4200	1529	675	224	25.03	4.92	10–78
Glyma.07G103600	Chr07:9945160..9951647	6488	2499	1578	525	57.9	8.94	67–128
Glyma.07G110200	Chr07:11240292..11244896	4605	2043	1263	420	47.16	6.97	15–72
Glyma.07G150700	Chr07:18133086..18137499	4414	1542	1041	346	37.6	9.85	4–67
Glyma.07G152900	Chr07:18633136..18637055	3920	2454	1743	580	63.73	9.74	31–92
Glyma.07G197600	Chr07:36595254..36599804	1551	2045	1470	489	54.28	8.99	75–135
Glyma.07G203800	Chr07:37320700..37321125	426	426	426	141	15.67	8.84	65–128
Glyma.07G244400	Chr07:42393536..42394912	1377	1041	750	249	28.79	10.20	41–102
Glyma.07G252300	Chr07:42987863..42992173	4311	3561	2877	958	108.92	6.76	67–128
Glyma.08G024300	Chr08:1936671..1938402	1732	546	546	181	20.68	8.15	5–55
Glyma.08G068300	Chr08:5241303..5244499	3197	2453	1368	455	50.31	8.09	68–130
Glyma.08G074200	Chr08:5668291..5669160	870	870	588	195	22.29	10.25	54–120
Glyma.08G109700	Chr08:8419650..8422508	2859	1037	561	186	21.6	10.21	51–115
Glyma.08G134400	Chr08:10299688..10307179	7492	1857	1314	437	47.12	9.45	82–143
Glyma.08G152100	Chr08:11680530..11688464	7935	1962	1335	444	48.95	8.81	89–151
Glyma.08G173900	Chr08:13878378..13884477	6100	2576	1689	562	64.65	8.47	296–360
Glyma.08G180100	Chr08:14426405..14426920	516	516	516	171	19.71	10.24	52–118
Glyma.08G180300	Chr08:14438331..14439308	978	978	516	171	19.74	10.24	52–118
Glyma.08G188900	Chr08:15140483..15144812	4330	2449	1914	637	73.08	8.76	95–174
Glyma.08G213400	Chr08:17225312..17230465	5154	1335	1335	444	48.28	8.25	65–126
Glyma.08G220000	Chr08:17875817..17877391	1575	1313	429	142	16.1	5.22	42–81
Glyma.08G238600	Chr08:20370125..20371352	1228	1145	741	246	28.19	7.18	102–165
Glyma.08G279900	Chr08:37918071..37919199	1129	1129	798	265	30.34	8.83	80–143
Glyma.08G295500	Chr08:41044066..41046731	2666	1582	870	289	33	9.88	5–72
Glyma.08G337100	Chr08:45406336..45408065	1730	1730	471	156	17.32	9.45	48–118
Glyma.09G003500	Chr09:293205..300873	7669	2015	1332	443	48.52	8.61	89–143
Glyma.09G032800	Chr09:2762138..2767670	5533	2900	2232	743	82.06	8.83	439–495
Glyma.09G041100	Chr09:3430561..3432082	1522	1005	813	270	31.63	9.98	45–98
Glyma.09G044000	Chr09:3755498..3761682	6185	2505	1077	358	41.09	9.50	99–152
Glyma.09G075400	Chr09:8193511..8201402	7892	2515	2058	685	76.7	5.31	99–153
Glyma.09G111100	Chr09:22005038..22006075	1038	558	558	185	21.41	6.24	129–181
Glyma.09G116600	Chr09:27016383..27022971	6589	1529	879	292	33.4	9.27	233–287
Glyma.09G116800	Chr09:27026697..27028223	1527	480	426	141	16.29	5.86	82–136
Glyma.09G133300	Chr09:33094816..33096668	1853	420	420	139	15.7	9.82	62–122
Glyma.09G155400	Chr09:37848195..37851767	3573	3441	2439	812	91.47	8.53	66–119
Glyma.09G208400	Chr09:43279596..43282064	2469	2469	1740	579	65.55	9.11	60–113
Glyma.09G283400	Chr09:49893145..49897583	4439	1772	1455	484	53.62	9.02	74–126
Glyma.10G014000	Chr10:1257860..1261280	3421	2069	1431	476	53.46	8.84	387–420
Glyma.10G094400	Chr10:13527590..13531121	3532	1312	846	281	32.47	9.11	31–83
Glyma.10G158200	Chr10:39215032..39216459	1428	876	876	291	32.31	9.34	60–123
Glyma.10G158300	Chr10:39221639..39223764	2126	1716	957	318	34.71	10.25	67–120
Glyma.10G216200	Chr10:44786403..44792509	6107	2076	1722	573	65.51	9.46	293–345
Glyma.10G252200	Chr10:48006799..48010531	3733	1479	918	305	35.77	9.75	39–92
Glyma.10G272200	Chr10:49433100..49438894	5795	1937	1233	410	45.34	6.54	18–72
Glyma.10G283300	Chr10:50391504..50394899	3396	1575	906	301	33.15	9.15	6–73
Glyma.11G032400	Chr11:2366022..2374465	8444	1581	1581	526	58.66	9.54	12–77
Glyma.11G050600	Chr11:3780408..3786583	6167	2990	1626	541	61.94	7.72	67–131
Glyma.11G077400	Chr11:5808747..5809882	1136	1136	477	158	17.42	9.75	64–128

Table 1 (continued)

Sequenced ID	Location	Sequence length			Protein			Position of J domain
		DNA (bp)	mRNA (bp)	CDS (bp)	Length (a.a.)	Mol.wt.(kD)	PI	
Glyma.11G095300	Chr11:7222140..7235534	13,395	4334	3477	1158	127.34	6.22	1017–1099
Glyma.11G102400	Chr11:7783752..7787262	3511	892	537	178	20.02	4.21	11–80
Glyma.11G105800	Chr11:8038613..8039501	889	889	306	101	11.69	9.04	3–67
Glyma.11G109700	Chr11:8359733..8362731	2999	1267	378	125	14.67	5.14	23–85
Glyma.11G241000	Chr11:33526493..33531210	4718	1958	1323	440	47.43	9.74	84–145
Glyma.12G001000	Chr12:77790..78816	1027	936	759	252	29.01	6.31	108–171
Glyma.12G015600	Chr12:1117363..1121163	3801	1107	372	123	14.25	4.64	11–73
Glyma.12G021400	Chr12:1535587..1546642	11,056	4393	3456	1151	126.78	5.89	1010–1092
Glyma.12G030700	Chr12:2284184..2285225	1042	1042	306	101	11.56	9.07	3–67
Glyma.12G095700	Chr12:8033041..8036166	3126	1961	1254	417	46.31	6.20	14–71
Glyma.12G117900	Chr12:12095819..12098847	3029	1543	1050	349	38.24	9.60	4–67
Glyma.12G130000	Chr12:14537935..14543293	5359	1407	999	332	37.32	6.96	66–128
Glyma.12G141300	Chr12:17716009..17716447	439	333	333	110	12.7	4.41	11–42
Glyma.12G168800	Chr12:32397292..32401606	4315	2316	1911	636	73.14	8.59	95–174
Glyma.12G189400	Chr12:35100214..35105956	5743	1350	753	250	29.96	9.88	42–95
Glyma.12G190100	Chr12:35168889..35171299	2411	1699	1254	417	46.34	6.25	14–71
Glyma.12G212100	Chr12:37114837..37119535	4699	1353	1020	339	38.25	7.32	71–133
Glyma.12G235500	Chr12:39449744..39456666	6923	1472	1020	339	38.06	6.69	7–68
Glyma.12G239500	Chr12:39830885..39838563	7679	1918	1332	443	48.63	8.85	89–151
Glyma.13G036700	Chr13:11480770..11486877	6108	1951	1149	382	43.63	6.81	6–68
Glyma.13G042000	Chr13:13452005..13456343	4339	3417	2316	771	87.52	9.68	66–127
Glyma.13G193900	Chr13:30714547..30714981	435	417	417	138	15.3	9	66–122
Glyma.13G200800	Chr13:31438634..31445721	7088	1784	1020	339	38.16	6.55	7–68
Glyma.13G214300	Chr13:32769353..32774554	5202	3806	2907	968	110.54	6.49	67–128
Glyma.13G235400	Chr13:34601529..34604996	3468	1458	1023	340	37.64	7.49	4–67
Glyma.13G235500	Chr13:34609107..34611350	2244	927	927	308	34.19	9.70	1–39
Glyma.13G257100	Chr13:36242651..36245265	2615	2615	1500	499	55.04	4.83	72–134
Glyma.13G289600	Chr13:38976043..38980726	4684	1459	1020	339	38.14	6.50	71–133
Glyma.13G311600	Chr13:40695198..40697649	2452	1758	1254	417	46.3	6.25	14–71
Glyma.13G312400	Chr13:40757045..40762412	5368	1353	753	250	29.93	9.88	42–95
Glyma.13G338600	Chr13:43110252..43113828	3577	1309	843	280	31.97	8.29	86–147
Glyma.13G366300	Chr13:45217310..45223538	6229	1502	1074	357	38.66	9.44	68–118
Glyma.14G008900	Chr14:679945..683405	3461	2930	2124	707	78.19	7.93	66–127
Glyma.14G010600	Chr14:817937..818830	894	894	429	142	15.96	8.98	40–103
Glyma.14G090500	Chr14:8255191..8260680	5490	2325	630	209	25.04	9.60	144–205
Glyma.14G118300	Chr14:15889765..15895675	5911	1625	1149	382	43.52	6.81	6–68
Glyma.14G178800	Chr14:43987725..44003499	15,775	2179	1410	469	52.7	8.65	83–145
Glyma.14G180400	Chr14:44324401..44328092	3692	961	417	138	16.59	4.46	40–102
Glyma.14G181600	Chr14:44444731..44447403	2673	1767	1095	364	40.44	9.06	91–153
Glyma.15G006900	Chr15:569216..577981	8766	1923	1482	493	53.36	8.78	67–128
Glyma.15G035700	Chr15:2836778..2840795	4018	1470	861	286	32.71	6.53	75–136
Glyma.15G057800	Chr15:4450904..4452397	1494	1494	1494	497	54.79	5.54	73–135
Glyma.15G077700	Chr15:5986404..5988453	2050	1411	1020	339	37.58	9.09	4–67
Glyma.15G077900	Chr15:5996630..5999931	3302	1478	1011	336	37.32	8.43	2–65
Glyma.15G098900	Chr15:7688068..7693423	5356	3809	2907	968	110.22	6.52	67–128
Glyma.15G137800	Chr15:11212212..11220821	8610	3079	2235	744	82.25	8.89	438–502
Glyma.15G146900	Chr15:12108503..12110387	1885	1406	813	270	31.56	9.94	41–102
Glyma.15G149100	Chr15:12287243..12293189	5947	1974	1086	361	41.51	9.04	103–164
Glyma.15G183400	Chr15:18240668..18247283	6616	2440	2058	685	76.67	5.30	99–161
Glyma.15G253300	Chr15:48178784..48185288	6505	3144	1686	561	64.62	8.41	295–359
Glyma.15G271500	Chr15:50871307..50878174	6868	1897	1335	444	48.97	8.80	89–151
Glyma.16G011500	Chr16:991887..995617	3731	1547	705	234	26.11	4.68	10–78
Glyma.16G041000	Chr16:3852109..3856099	3991	858	858	285	31.85	8.42	54–115

Table 1 (continued)

Sequenced ID	Location	Sequence length			Protein			Position of J domain
		DNA (bp)	mRNA (bp)	CDS (bp)	Length (a.a.)	Mol.wt.(kD)	PI	
Glyma.16G097000	Chr16:18799491..18800362	872	207	207	68	7.72	10.59	31–65
Glyma.16G127600	Chr16:27950347..27950844	498	498	498	165	19.02	9.85	66–130
Glyma.16G127700	Chr16:27974774..27975479	706	706	474	157	17.56	9.49	61–125
Glyma.16G205900	Chr16:36650239..36655749	5511	3686	2340	779	87.12	9.37	66–127
Glyma.17G022200	Chr17:1605507..1609543	4037	3460	3135	1044	118.44	5.95	151–212
Glyma.17G029500	Chr17:2172877..2174369	1493	1097	807	268	31.03	10.19	40–93
Glyma.17G078100	Chr17:6096537..6099731	3195	2329	1881	626	71.58	4.84	10–68
Glyma.17G120500	Chr17:9587225..9604568	17,344	8509	7752	2583	282.4	5.78	1544–1585
Glyma.18G016200	Chr18:1156405..1160754	4350	2067	1323	440	47.57	9.54	84–145
Glyma.18G072300	Chr18:6818985..6820432	1448	1448	456	151	16.68	9.46	48–113
Glyma.18G127500	Chr18:17096119..17098853	2735	1663	870	289	32.89	9.85	5–74
Glyma.18G146200	Chr18:24753304..24754749	1446	1446	783	260	29.65	8.55	76–139
Glyma.18G158500	Chr18:35328857..35329255	399	399	399	132	14.78	7.07	59–123
Glyma.18G198900	Chr18:47710563..47710854	292	292	228	75	8.72	5.02	5–29
Glyma.18G201600	Chr18:48163734..48168274	4541	1544	1020	339	37.31	9.73	4–67
Glyma.18G204000	Chr18:48677255..48680846	3592	2159	1734	577	63.56	9.84	31–92
Glyma.19G063100	Chr19:13580082..13582867	2786	1234	924	307	35.05	7.59	55–115
Glyma.19G064700	Chr19:16056899..16061356	4458	1328	549	182	20.44	9.75	2–69
Glyma.19G112100	Chr19:36610814..36614632	3819	1292	924	307	34.81	8.06	57–118
Glyma.19G143100	Chr19:40408474..40411444	2971	1296	837	278	32.02	7.34	23–86
Glyma.19G148000	Chr19:40867988..40872227	4240	1239	765	254	29.55	9.89	196–250
Glyma.19G180600	Chr19:43944097..43949261	5165	2046	1509	502	55.18	6.27	373–436
Glyma.19G213500	Chr19:46690678..46692181	1504	699	411	136	15.82	8.43	7–59
Glyma.19G215100	Chr19:46807027..46811823	4797	1947	1032	343	38.85	6.60	26–88
Glyma.19G215400	Chr19:46837821..46841361	3541	2445	1713	570	63.59	9.04	395–429
Glyma.19G229700	Chr19:48069374..48070638	1265	875	495	164	18.55	5.07	12–79
Glyma.19G239700	Chr19:48790745..48796215	5417	4598	3177	1058	118.64	9.19	67–128
Glyma.20G002400	Chr20:235327..239941	4615	1711	1494	497	55.15	9.17	76–136
Glyma.20G013600	Chr20:1214020..1216156	2137	1125	525	174	19.95	4.81	11–77
Glyma.20G020700	Chr20:2131066..2131518	453	453	453	150	16.45	5.86	41–75
Glyma.20G024300	Chr20:2640491..2641462	972	972	330	109	11.96	9.55	60–107
Glyma.20G106400	Chr20:34891407..34893605	2199	1531	915	304	33.7	9.08	6–73
Glyma.20G117900	Chr20:36067233..36080533	13,301	1944	1233	410	45.35	6.40	18–80
Glyma.20G141300	Chr20:38004325..38007997	3673	1429	918	305	35.71	9.75	39–100
Glyma.20G175700	Chr20:41306195..41313315	7121	2239	1593	530	60.37	6.52	291–339
Glyma.20G230400	Chr20:46445459..46448417	2959	2678	2130	709	78.74	8.57	67–128
Glyma.U012100	scaffold_21:489990..492974	2985	1889	1254	417	46.3	6.20	14–71

Exon/intron organization analysis and chromosomal locations of DnaJ family genes

It is widely believed that exon/intron structural divergences have a crucial impact on the evolution of multiple gene families (Xu et al. 2012). Paralogous genes always have near resemblance in exon/intron organization (Rogozin et al. 2005). By analyzing gene structure, we can get some information about the evolutionary mechanism underlying the genesis of gene families (Zhao et al. 2016). Therefore, to further understand the structural diversity of DnaJ family genes, we investigated the exon/intron organization by comparing the CDS sequences with their corresponding genome sequences of individual DnaJ genes in soybean (Fig. 3). According to the analysis result, we found that the majority of gene pairs exhibited highly conservation, such as the exon numbers and exon length. The exon numbers in type I and type III have considerable variation between these two groups, meaning these two types of DnaJ genes have different tendency from origin by gaining or losing intron. In general, the similar exon/intron distributions were presented in the same phylogenetic group, suggesting soybean DnaJ had undergone gene duplications during the evolutionary processes.

As shown in Fig. 4, 195 of the 196 soybean DnaJ genes are widely but biasedly distributed on a total of twenty

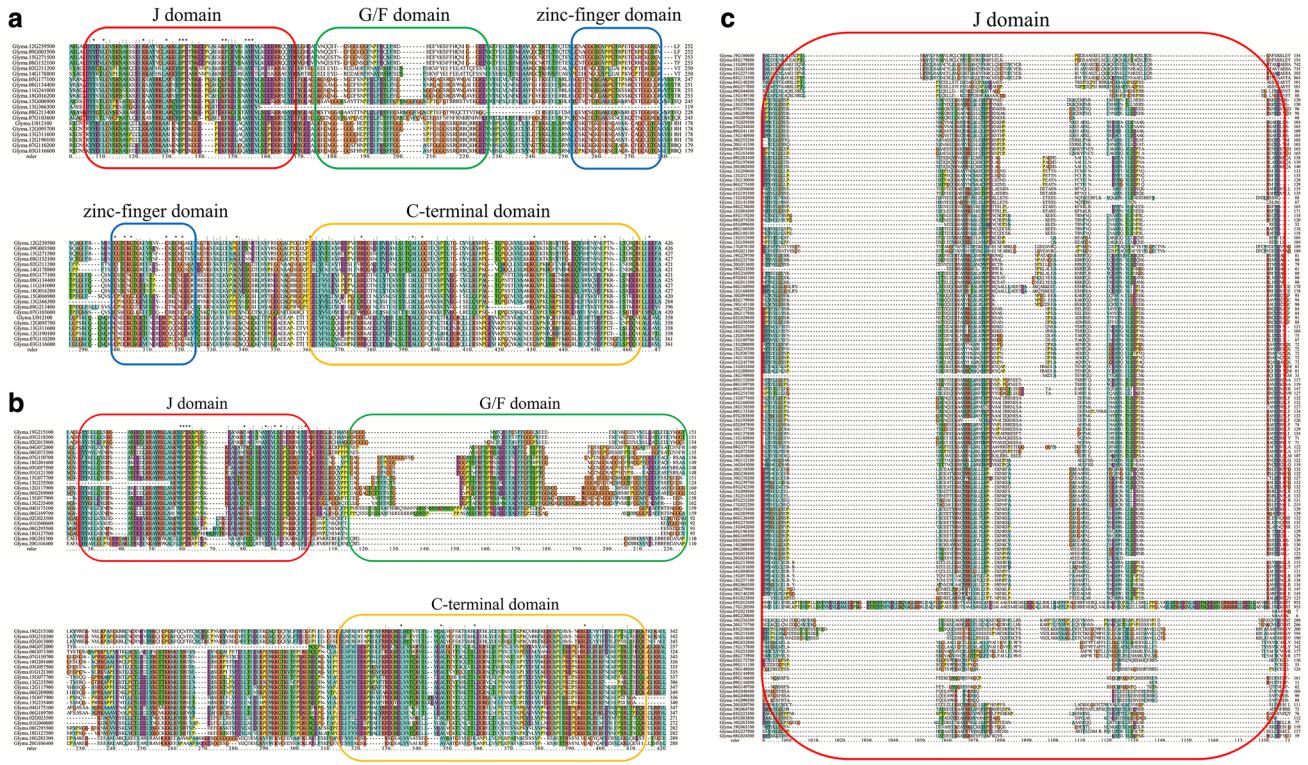

Fig. 1 Multiple sequence alignments of soybean DnaJ family members. Multiple sequence alignments of type I (**a**), type II (**b**) and type III (**c**) DnaJ proteins were performed by ClustalX2.0 program. Conserve domains of each type of DnaJ were marked with *colored box*. (Color figure online)

soybean chromosomes, only one gene (*Glyma.U012100*) is mapped on the unattributed scaffold. The number of DnaJ genes in each chromosome is various. Chromosome 17 has only 4 soybean DnaJ genes while chromosomes 8, 12 and 13 have 18, 15 and 14 DnaJ genes, respectively. Moreover, we found that some chromosomal regions have dense distribution of DnaJ genes, such as the end of chromosome 3, 13 and the center of chromosome 8. However, no substantial clustering of soybean DnaJ genes was exhibited on the map.

Differential expression profiles of *G. soja* DnaJ genes under alkaline stress

Abiotic stresses can obviously inhibit the growth, development and yield of most crop plants (Jose and Thomas 2015). Previous studies reported that the expression of DnaJ genes could be induced by multiple environmental stresses, such as salinity, high and low temperature, and oxidative stresses. However, we still knew a little about the functions of DnaJ proteins in alkaline stress. For this reason, we explored the whole DnaJ gene family expression profiles under 50 mM $NaHCO_3$ (pH 8.5) in *G. soja* G07256 using our previous RNA-seq data (Fig. 5a). Amongst them, 27 DnaJ genes (no sequence in type I, *Glyma.18G127500* in type II and the others 26 sequences in type III) exhibited differential expressions upon alkaline stress. Notably, we noticed from heat map that the majority of differently expressed genes were distributed to type III DnaJ genes. Thus, we inferred type III J-proteins were mostly involved in response to alkaline stress. We also found that four type III DnaJ genes had similar expression profiles and showed significantly increased transcript levels at early time point (3 h) after $NaHCO_3$ treatment. Coincidentally, those genes were neighbors with each other according to the phylogenetic tree (Fig. 5a). Therefore, we chose one representative gene, *GsJ11* (*Glyma.11G077400*), which was highly induced by $NaHCO_3$ treatment for further functional dissection.

Spatial expression pattern of *GsJ11* and its response to bicarbonate alkali stimuli in *G. soja*

To determine the spatial expression patterns, we measured the endogenous *GsJ11* expression levels in root tip, stem, young leaf, old leaf, seed, pod and flower of *G. soja* using quantitative real-time PCR (Fig. 5b). As shown in Fig. 5b, *GsJ11* was widely expressed in all vegetative and reproductive tissues and organs. *GsJ11* had a high expression levels

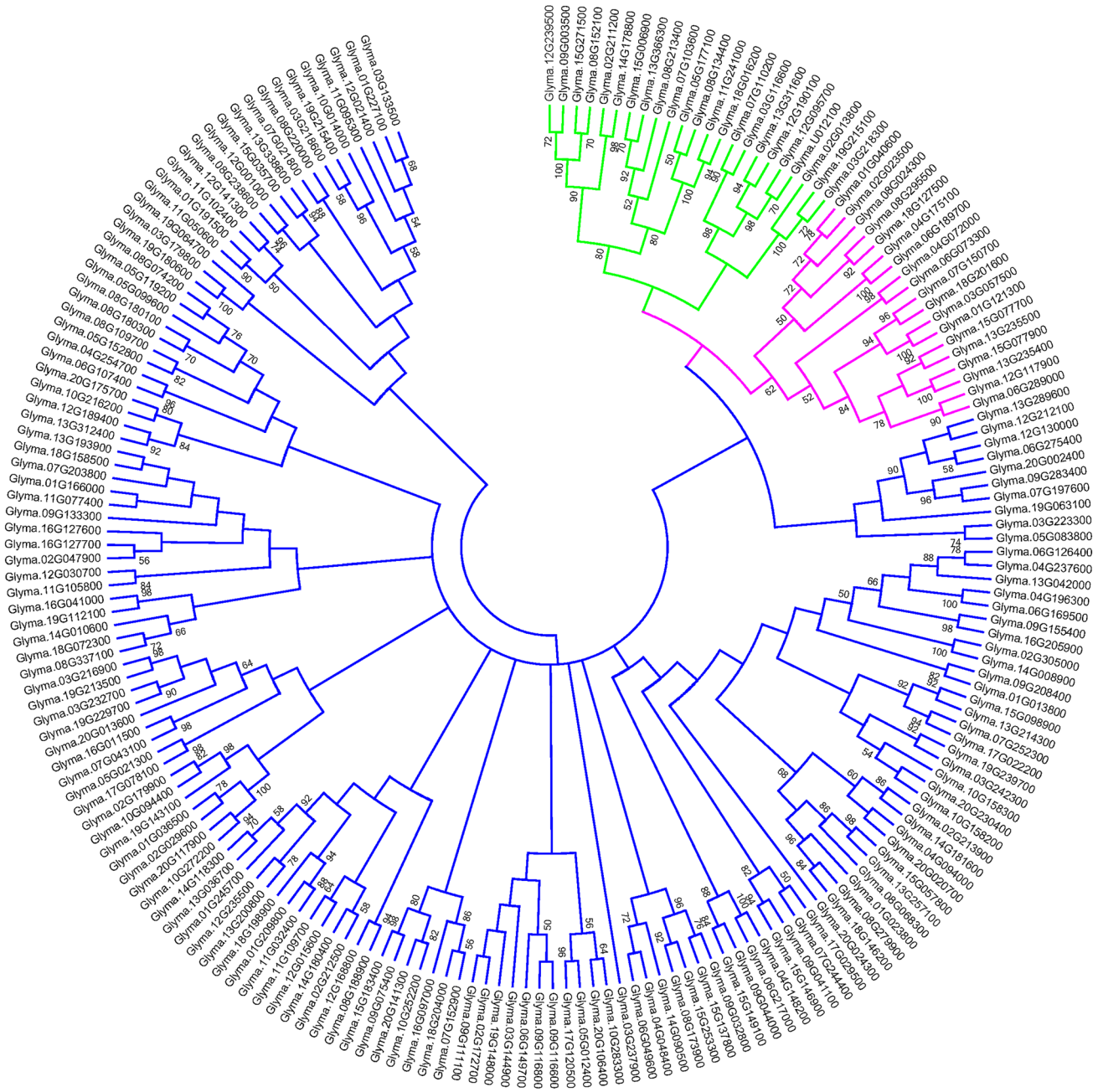

Fig. 2 Phylogenetic analysis of DnaJ family proteins. A phylogenetic tree was constructed by using MEGA 5.0 to determine evolutionary distance among the members of DnaJ protein family of *Glycine max*. The maximum likelihood (ML) method was used for construction of the tree and the reliability of the branches was inferred from a bootstrap analysis of 500 replicates. Each cluster was indicated by a specific color, type I, type II and type III were marked in *green*, *pink* and *blue*, respectively. (Color figure online)

in young leaf and flower but moderate expression levels in root tip, seed and pod.

To examine the response of *GsJ11* to bicarbonate alkali, qRT-PCR were carried out using the RNA samples extracted from the root tips of 21-d-old *G. soja* 07256 seedlings treated with 50mM $NaHCO_3$ for different time durations. Consistent with our previous RNA-seq data, the transcript accumulation of *GsJ11* was obviously increased after treatment (Fig. 5c). Specifically, the transcript level of *GsJ11* maximized with more than twofold increase at 3 h and then dropped down to normal level, implicating that *GsJ11*is actively responsive to bicarbonate alkaline stress at early stage.

Fig. 3 Exon/intron organization structure of soybean DnaJ family genes. Schematic diagram for exon/intro structures of 196 DnaJ family genes identified from soybean. Diagram was generated by GSDS online tool using coding sequences and corresponding genome sequences. *Yellow boxes, blue boxes* and *lines* represent exons, upstream/downstream and introns, respectively. The sizes of exons and introns can be estimated using the scale at the bottom. (Color figure online)

Ectopic expression of *GsJ11* enhances plant tolerance to $NaHCO_3$

To investigate the physiological function of *GsJ11* gene,we ectopically expressed *GsJ11* controlled by CaMV35S promoter in *Arabidopsis*. Three homozygous T_3 OX transgenic *Arabidopsis* lines (#1, #2, #3) were generated and selected for further study. By contrast, we obtained one *AtJ11* (*At4G36040*) T-DNA insertion lines from TAIR (SALK_015630 C). The homozygous mutant line, *atj11*, was authenticated by T-DNA border primers and gene-specific primers (Fig. 5d). We confirmed that expression of endogenous *AtJ11* was abolished in mutant line whereas it was present in WT and *GsJ11* OX lines using semi-quantitative RT-PCR using *AtJ11* gene-specific primers (Fig. 5e up). Meanwhile, we identified the transcription abundance of each *GsJ11* OX line by semi-quantitative RT-PCR using *GsJ11* gene-specific primers (Fig. 5e down). The analysis result confirmed that these transgenic lines were independent and had high enough exogenous *GsJ11* expression levels to function. However, the WT and mutant plants did not show any *GsJ11*expression.

To determine the physiological functions of GsJ11 under alkaline condition, we examined the effect of J11 on seed germination. The WT, OX and *atj11* mutant seeds were germinated on 1/2 Murashige and Skoog (MS) solid media

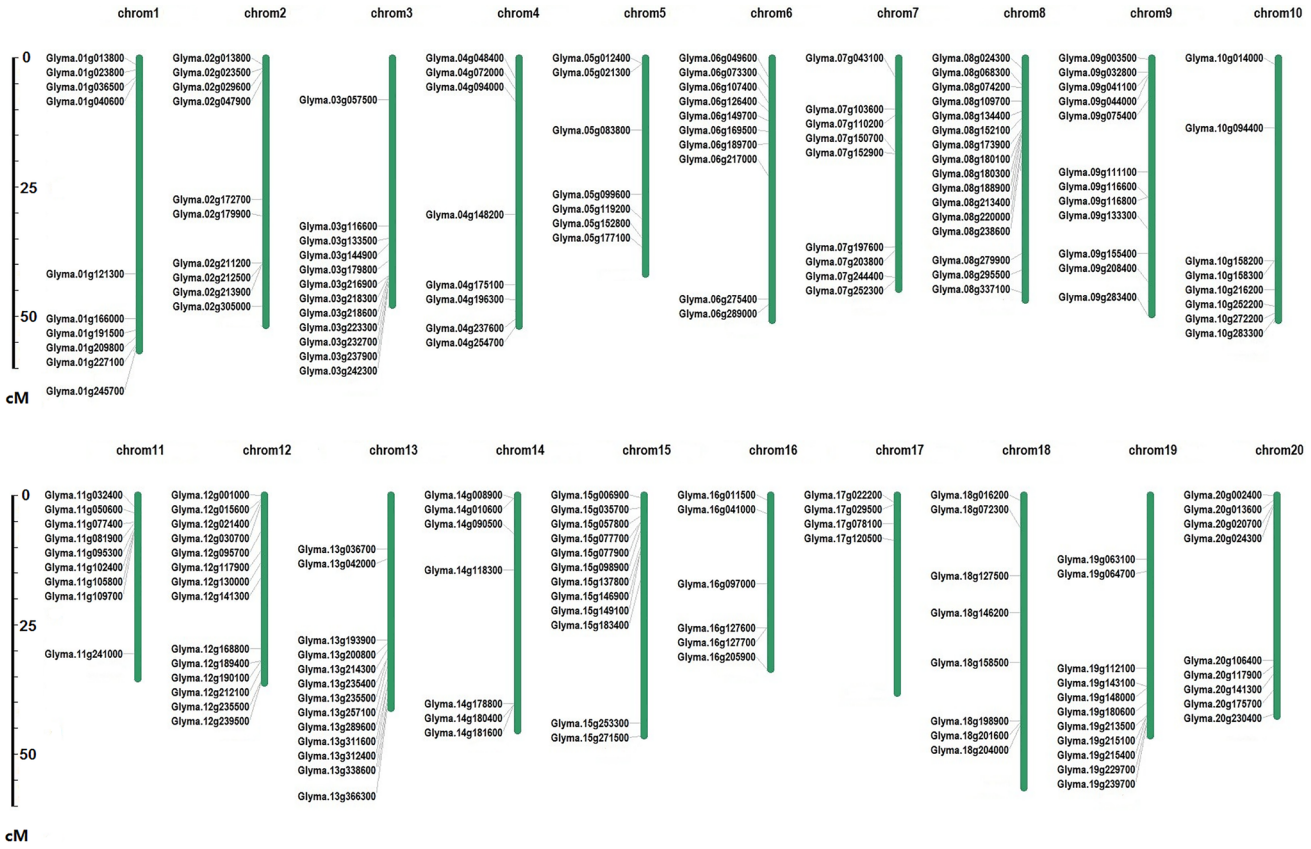

Fig. 4 Chromosomal locations of DnaJ family genes in soybean. Chromosomal locations of soybean DnaJ family genes on all 20 chromosomes were performed by using MapInspect software. The chromosomes are represented by *green bars* and the numbers of chromosomes are shown at the *top* of each bar. The scale on the *left* of the image represents the length of the chromosome. (Color figure online)

containing 0, 6, 7 and 8 mM $NaHCO_3$, respectively. Without $NaHCO_3$ treatment, each line seeds showed similar and rapid seed germination and young seedling growth (Fig. 6a). However, on the media containing $NaHCO_3$, the seed germinations were generally inhibited. On medium with 6 mM $NaHCO_3$, the germination rates of all lines were significantly decreased in early stage, but the seed germination rate of *GsJ11* OX lines were significantly higher than WT and *atj11* mutant lines under the same condition after 5 days of seed sowing. The germination percentages were nearly 50% for mutant line and 60% for the WT, whereas 80–90% for the OX seeds. This trend was even more pronounced in the presence of higher $NaHCO_3$ concentrations (Fig. 6a, b).

To further determine if *GsJ11* overexpression can enhance plant tolerance to $NaHCO_3$, 7-day-old seedlings of each line grown on the normal medium were transferred to media containing 0, 6 or 7 mM $NaHCO_3$ and were continued to grow for 6 days. The seedlings on the normal medium did not show obvious difference of root elongation among WT, *GsJ11* OX and *atj11* mutant lines (Fig. 7a). However, on medium containing 6mM $NaHCO_3$, the root elongation of *atj11* was significant inhibited compared to WT, and this reduction in root development was more pronounced in the presence of 7 mM $NaHCO_3$ (Fig. 7a, b). However, ectopic expression of *GsJ11* (OX lines #1, #2 and #3) could significantly promote root elongation (Fig. 7a, c). These results suggested that GsJ11 can enhance plant resistance to $NaHCO_3$.

To provide more evidence for our discovery, we treated the adult seedlings of WT, *atj11*, three *GsJ11* OX lines with $NaHCO_3$. 4-week-old plants of each line grown in soil were irrigated with 150 mM $NaHCO_3$ solution every 3 days for total 14 days. Consistent with the observations from young seedlings, all lines exhibited similar growth in the pots irrigated with water (Fig. 8a) but their phenotypes demonstrated significant differences after irrigation with $NaHCO_3$ solutions for the indicated time. All of the *GsJ11* OX lines had stronger growth, higher survival rate and more green leaves than the WT. However, the mutant line was the worst and most plants turned yellow even dead after treatment (Fig. 8a). To further confirm our observation, the total chlorophyll contents of all lines were measured. As shown in Fig. 8b, the chlorophyll contents were generally decreased in all lines after $NaHCO_3$ treatment, but *GsJ11*

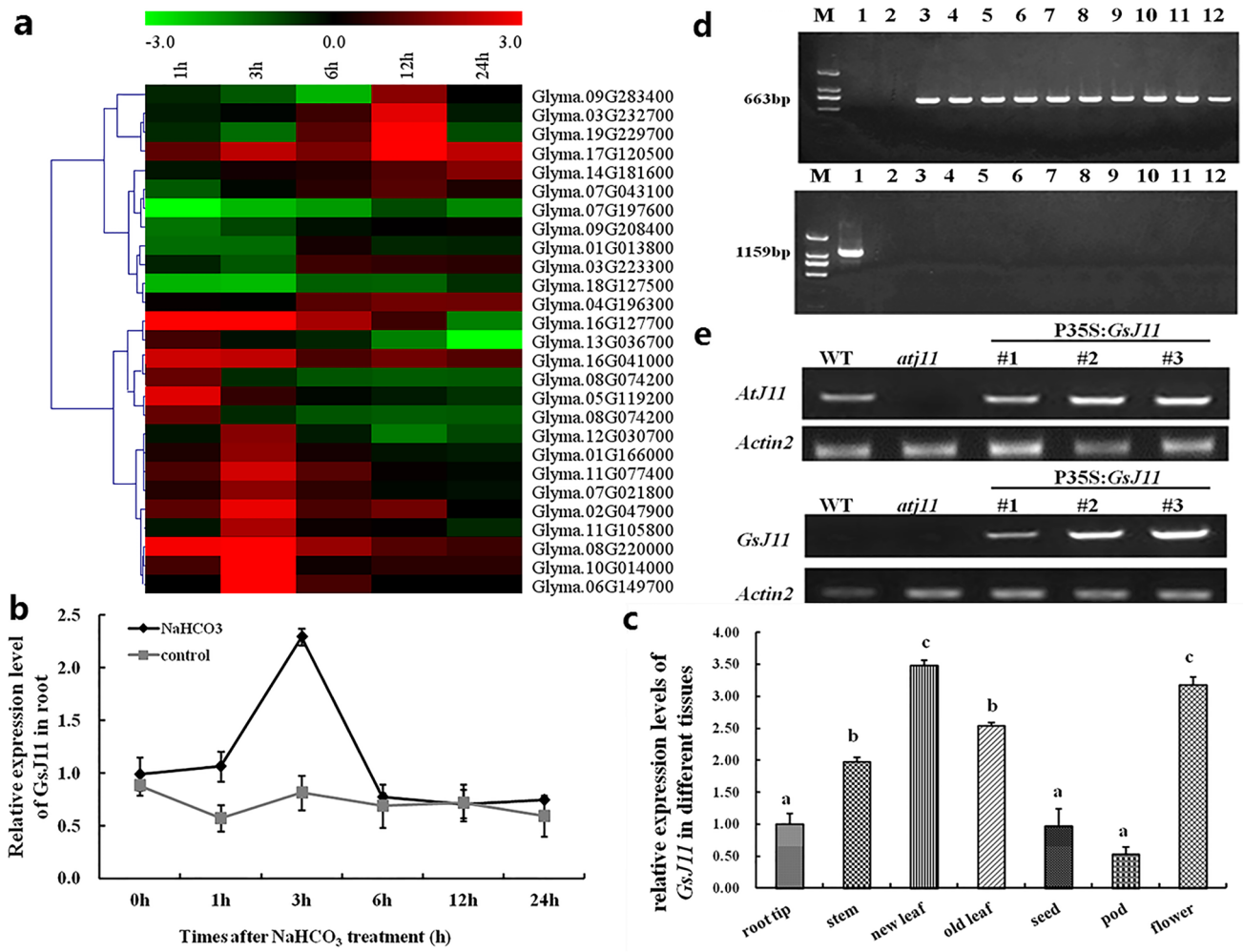

Fig. 5 Differential expression profiles of *GsJ11*and characteristics of OX lines and mutant lines. **a** Expression profiles of DnaJ genes in *G. soja* roots under 50 mM $NaHCO_3$ treatment according to the RNA-seq data. The *color scale* represents genes log2 fold changes (LogFC) to 0 h. *Red and green squares* represent high or low levels of transcript abundance compared with 0 h, respectively. **b** The spatial expression of *GsJ11* was detected in various tissues of wild soybean. **c** Relative expression analysis of *GsJ11* induced by $NaHCO_3$ revealed by qRT-PCR. **d** Identification of *atj11* T-DNA insertion mutant. *Lane 1* was WT sample and *lane 2* was distilled water; *lane 3–12* was *atj11* mutant samples. **e** Expression levels of endogenous *AtJ11* and *GsJ11* in WT, *atj11* mutant and three *GsJ11* overexpressed lines, respectively. (Color figure online)

OX lines still had relatively the highest pigment contents among the WT and *atj11* lines. More specifically, the mean value of chlorophyll contents was 79.73 (μg/g FW) in wild type, and 70.31 (μg/g FW) in mutant line, while the value of OX lines were from 86.48 to 93.28 (μg/g FW). Moreover, it is widely accepted that malondialdehyde (MDA) is generated by peroxidation process of membrane lipid, and high MDA level can lead to damage of cell membrane, so MDA is usually seen as an indicator to measure oxidative damage (Wang et al. 2016; Weber et al. 2004). We then determined the MDA contents in all plants with normal and alkaline treatments. The data showed that MDA levels in WT and *atj11* lines were much higher than *GsJ11* OX lines (Fig. 8c). For example, the MDA contents in WT and mutant lines were approximately 40 (μmol/g FW) under $NaHCO_3$ treatment, whereas the MDA contents in *GsJ11* OX lines were only half or less. These results support our conclusion that *GsJ11* enhances plant $NaHCO_3$ tolerance while loss of *J11* increases sensitivity to $NaHCO_3$.

Expression patterns of abiotic stress-responsive marker genes

It is suggested that alkaline stresses induce the expression of numerous relative stress-inducible genes in the progress of plant adaptation (Alhendawi et al. 1997). For a further understanding about the role of *GsJ11* in plant tolerance to $NaHCO_3$, we measured the transcript levels

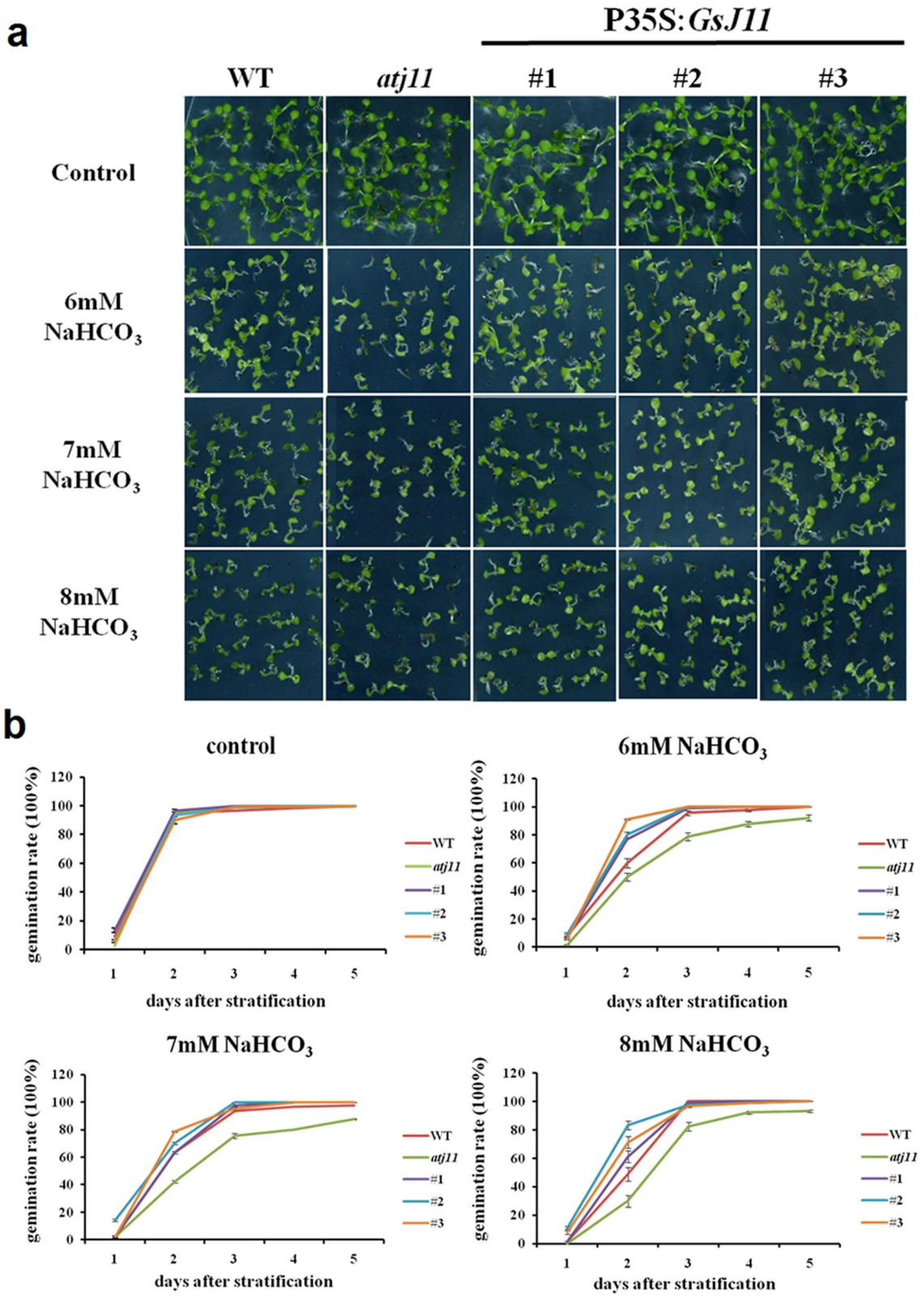

Fig. 6 Ectopic expression of *GsJ11* enhances plant tolerance to $NaHCO_3$ during the seed germination stage. **a** The growth performance of WT, *GsJ11* OX and *atj11* seedlings on medium containing 0, 6, 7 or 8 mM $NaHCO_3$, respectively. **b** Seed germination rates of WT, *GsJ11* OX and *atj11* lines

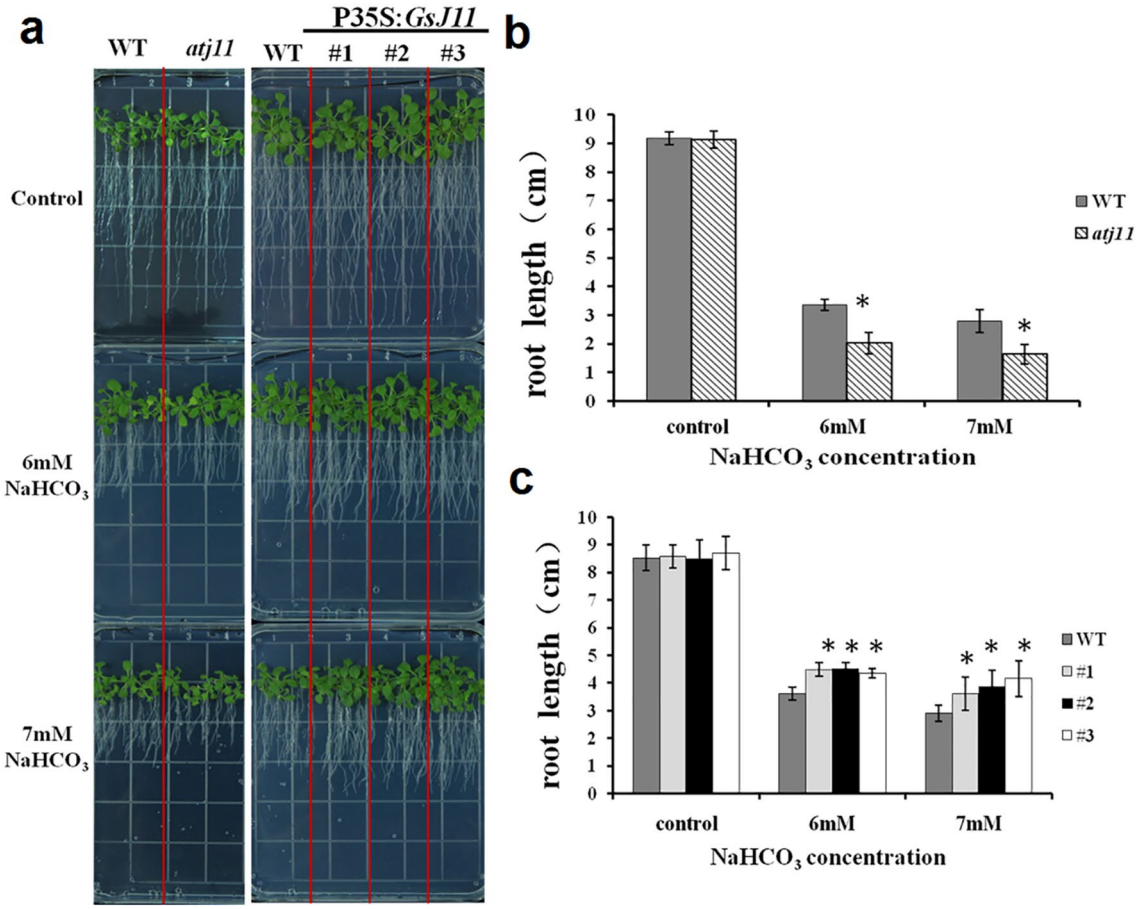

Fig. 7 Ectopic expression of *GsJ11* promotes seedling root elongation under $NaHCO_3$ treatment. **a** Phenotypes of WT, *atj11* and *GsJ11* OX seedlings under normal and alkaline stress. **b** Primary root length of WT and *atj11* seedlings. **c** Primary root length of WT and *GsJ11* OX seedlings. *P < 0.05; **P < 0.01 by Student's *t* test

of seven stress-inducible genes (*NADP-ME, H^+-ATPase, H^+-PPase, KIN1, RD29A, COR47* and *RD22*). The results of qRT-PCR showed the expressions of all selected genes were rapidly and significantly induced by $NaHCO_3$ treatment in WT and OX lines, however these marker genes showed low induction in the mutant line (Fig. 9). *H^+-ATPase, H^+-PPase, NADP-ME, RD29A* and *KIN1*were significantly regulated in OX lines than in wild type. Although the transcription levels of *COR47* and *RD22* also increased, there were no significant differences between all lines. In summary, these qRT-PCR analyses suggested that *GsJ11* promoted bicarbonate resistance by regulating the expression of relative stress-induced gene, and deletion of J11 caused low responses of those genes.

Discussion

Proteins are always at the risk of losing their functional conformation due to various environmental stresses in the native conditions. Molecular chaperones can keep proteins in proper conformations by facilitating the folding or refolding of the misfolded proteins. Heat shock 70 kDa proteins (Hsp70s) are known as a kind of ubiquitous chaperones which participate in a myriad of biological processes (Bukau et al. 2006; Hartl and Hayer-Hartl 2009). Many protein folding and refolding are driven by a diverse class of cofactors: DnaJ (Kampinga and Craig 2010). In this study, we focused on the diversity of this large DnaJ family in soybean genome, identified and characterized an alkaline stress-responsive gene *GsJ11* based on genome-wide analysis.

Previous reports have revealed the complexity and diversity of DnaJ gene family in *Arabidopsis*, rice and yeast (Rajan and D'Silva 2009; Sarkar et al. 2013; Walsh et al. 2004a). In this study, we identified 196 non-redundant DnaJ genes in soybean genome (Table 1) compared to 116 DnaJ genes in *Arabidopsis* and 104 DnaJ genes in rice. Depending on the presence of conserved domain, DnaJ protein family could be divided into three clusters

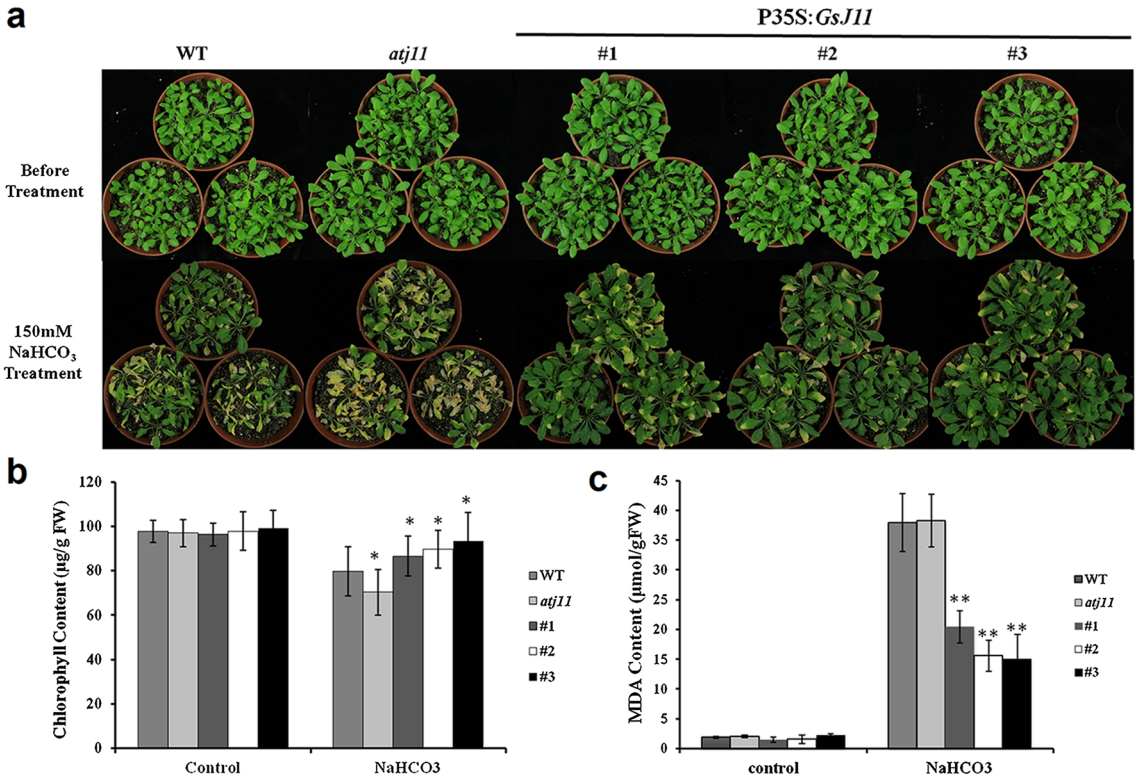

Fig. 8 *GsJ11* enhances plant tolerance to $NaHCO_3$ at the adult stage. **a** Phenotypes of WT, *GsJ11* OX and *atj11* plants in response to alkali at adult stage. **b** The total chlorophyll contents of WT, *GsJ11* OX and *atj11* plants. **c** The total MDA contents of WT, *GsJ11* OX and *atj11* plants. *P < 0.05; **P < 0.01 by student's *t* test

(Walsh et al. 2004b). Similar with *Arabidopsis* and rice, all types of DnaJ proteins were detected in soybean based on their structures (Online Resource 2). For example, the proteins in the same clusters share the same domain architectures, implicating the proteins within one cluster should have similar functions and each type of J proteins are crucial and play different roles in cellular processes.

All of the J proteins contain a highly conserved signature J domain (Cyr et al. 1992). As shown in multiple sequence alignments, the J domain are generally located in the N-termini of DnaJ proteins and are highly exhibited sequence conservation, and a highly conserved HPD motif is existed between helix II and helix III in all J domains (Fig. 1), suggesting that the J domain and HPD motif are necessary for a J protein to carry out its function.

Strikingly, according to the phylogenic tree, we found the number of each cluster members is different; the members in type III are significantly more than those in the other two types (Fig. 2). These phenomena were also found in other species, such as rice and *Arabidopsis* (Sarkar et al. 2013). Thus, we hypothesized that type III J proteins are widely involved in cellular physiological processes by more flexible modes. On the other hand, the exon/intron organization analysis also confirmed that type I and III DnaJ genes have considerable variation in distribution (Fig. 3). Whereas the genes in same phylogenetic branch have consistent exon numbers and lengths, suggesting DnaJ genes had undergone gene duplication in evolution.

There is plenty of evidence that DnaJ genes can be induced by multiple abiotic stresses, such as heat, cold, wounding or high-salinity (Kong et al. 2014, So et al. 2013). For example, a tomato chloroplast-targeted DnaJ protein, SICDJ2, could enhance plants tolerance to heat stress by protecting Rubisco activity (Wang et al. 2015). Three small type III DnaJ proteins were involved in optimization of photosynthetic reaction during high light condition (Chen et al. 2010). Furthermore, the *Arabidopsis* chaperone J3's expression could be induced to salt at alkaline pH (Yang et al. 2010). However, only few focus on bicarbonate stress. Thus, we explored the expression profiles of *G. soja* DnaJ genes under 50 mM $NaHCO_3$ based on RNA-seq data (Fig. 5a). We obtained 27 significant differential expressed genes out of 196 DnaJ genes. Notably, 26 in those differential expressed genes were distributed in type III, so we postulate that these abiotic-responsive DnaJ genes are majorly concentrated in type III and play crucial roles against abiotic stresses in plants.

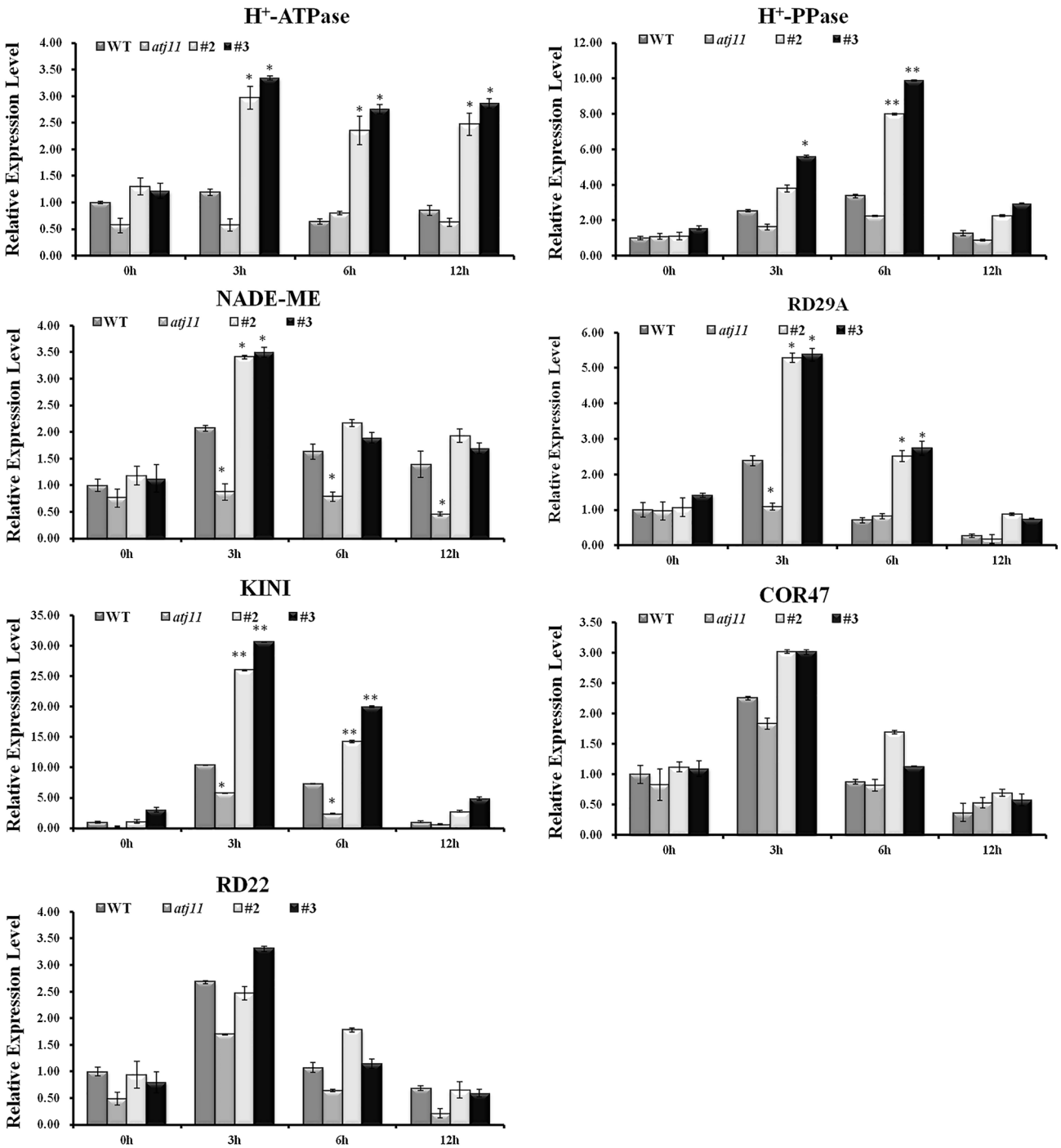

Fig. 9 Expression patterns of abiotic stress-responsive marker genes. Transcript levels of stress-inducible marker genes in WT, *GsJ11* OX and *atj11* seedlings determined by qRT-PCR. *Actin2* gene was used as an internal control. *Error bars* represent standard deviations (SD) of three independent biological repeats and three technical repeats. *P < 0.05; **P < 0.01 by Student's *t* test

In this paper, we concentrated on a novel type III DnaJ family gene from *G. soja, GsJ11*, which was rapidly induced by bicarbonate stress according to our RNA-seq data. Here, we detected the inducible expression patterns of *GsJ11* in *G. soja* root during $NaHCO_3$ treatment as shown by qRT-PCR result (Fig. 5c), coinciding with our previous findings of the other alkaline-induced genes (Liu et al. 2015; Yu et al. 2016). To further evaluate the function of *GsJ11* in response to alkaline condition, gain-of-function of *GsJ11* plants and loss-of-function mutants of its

homologous gene in *Arabidopsis* were generated for phenotypic analyses. Compared to neutral salts, alkaline salt stress has more inhibitory effect on seed germination and physiological characteristics. As expected, the plants with ectopic expression of *GsJ11* exhibited greater alkali tolerance than the wild-type plants, such as higher germination rates (Fig. 6a, b), less root elongation inhibition (Fig. 7a–c), higher survival rates (Fig. 8a), higher chlorophyll contents (Fig. 8b) and much lower MDA contents (Fig. 8c). By contrast, *atj11* mutant line displayed completely opposite phenotypes. Taken together, those evidences strongly suggest *GsJ11* facilitates alkaline tolerance in plants. Furthermore, we also found that the transgenic lines with more transcripts (Fig. 5e) have greater tolerance (Figs. 6, 7, 8). Namely, the alkaline resistance of *GsJ11* overexpressing line is positively correlated with its abundance of GsJ11 transcripts.

Evidence has been provided that most of bicarbonate-induced genes are involved in metabolism, signal transduction and transcription (Alhendawi et al. 1997). It has been reported that NADP-MEI, NADP-MEII and V-H^+-PPase are highly responsive to bicarbonate stress and can prevent plant cells from the damage of environmental stress by regulating intracellular pH (Fushimi et al. 1994). In this study, we detected the transcription levels of three bicarbonate-response marker genes, including *H^+-ATPase, H^+-ATPase* and *NADP-Me* in *GsJ11* OX, WT and *atj11* lines, respectively (Fig. 9). We also explored other stress-regulated genes such as *RD29A, KINI* and *COR47*, which could be significantly induced by drought, cold and ABA (Kurkela and Franck 1990; Seki et al. 2003; Wang et al. 1995). And we found that the transcript levels of those genes in *GsJ11* OX lines were rapidly up-regulated after alkaline treatment compared with WT and *atj11* lines. *H^+-ATPase, H^+-PPase, NADP-ME, RD29A* and *KIN1* were strongly up-regulated in *GsJ11* OX lines than WT line, *COR47* and *RD22* did not exhibit obvious difference between *GsJ11* OX and WT lines although their expression levels were also increased. These results suggested that *GsJ11* may participate in alkali stress signaling transduction by regulating genes expression and subsequently enhances alkaline resistance in plants.

Based on emerging research, DnaJs participate in some essential biochemical pathways in plant cell. We have known that J3 activates PM H^+-ATPase activity by repressing PKS5 kinase activity (Yang et al. 2010). A type III J-protein in *Arabidopsis*, J20, interacts with DXS enzyme, the first enzyme of MEP pathway and identifies unfold or misfolded form of DXS and target them to the Hsp70 system for proper folding under normal conditions or degradation upon stress conditions (Pulido et al. 2013). Two other small chloroplast-targeted J-protein, J11 and J8 participate in stabilization of PSII complexes and are involved in the folding or assembly processes of Rubisco. Moreover, *LeCDJ1*, plays a similar role in the maintenance of PSII activity under abiotic stress (Kong et al. 2014). A chloroplast Hsp70 could directly interact with SlCDJ2, two component function together in preventing Rubisco protein under stress conditions(Wang et al. 2015). Thus, we speculate that GsJ11 has a similar function pattern in the response to alkaline stress. The plant growth in alkaline soil is severely inhibited due to impaired chlorophyll synthesis and root respiration. GsJ11 may identify particular client protein (Hsp70) and help them recover proper conformation, sequentially improve the stability of the composites, such as PSII complexes and respiratory chain, finally maintain the normal physiological and biochemical functions in alkaline stress.

In addition, the spatial expression analysis showed that *GsJ11* had highly expression levels in young leaf and flower besides root (Fig. 5b). In *Arabidopsis*, a type III J protein AtDjC17 caused altered root hair development (Petti et al. 2014). Those evidences provided a clue that type III DnaJ proteins may also play roles in plant development process.

In conclusion, we defined systematic diversity of soybean DnaJ gene family and found type III DnaJ proteins are involved in response to abiotic stresses. Here we identified a novel type III DnaJ gene, *GsJ11*, from *G. soja*, and confirmed it can enhance plant tolerance to bicarbonate stress. Furthermore, the precise function and the mechanism of GsJ11 were investigated at the present of $NaHCO_3$. Our results provide references for further studies on family biological functions of DnaJ proteins.

Acknowledgements This work was supported by National basic scientific talent training fund projects (J1210069), and the starting grant of NEAU to Xiaodong Ding.

Author contributions Xuewei Song and Yanming Zhu designed the research; Xuewei Song, Yang Yu, Chao Chen, Pinghui Zhu, Ranran Chen, Xiangbo Duan, Huiqing Li and Lei Cao performed the experimental assays; Huizi Duanmu, Qiang Li and Xiaoli Sun contributed with the data analysis and figures design; Xuewei Song drafted the manuscript; Zaib un Nisa and Xiaodong Ding revised the manuscript. All authors contributed to editing and approving the final version of the manuscript.

Compliance with ethical standards

Conflict of interest The authors declare that they have no conflict of interest related to the work described in this manuscript.

References

Alhendawi RA, Römheld V, Kirkby EA, Marschner H (1997) Influence of increasing bicarbonate concentrations on plant growth, organic acid accumulation in roots and iron uptake

by barley, sorghum, and maize. J Plant Nutr 20:1731–1753 doi:10.1080/01904169709365371
Bekh-Ochir D et al (2013) A novel mitochondrial DnaJ/Hsp40 family protein BIL2 promotes plant growth and resistance against environmental stress in brassinosteroid signaling. Planta 237:1509–1525. doi:10.1007/s00425-013-1859-3
Bie Z, Ito T, Shinohara Y (2004) Effects of sodium sulfate and sodium bicarbonate on the growth, gas exchange and mineral composition of lettuce. Scientia Horticulturae 99:215–224 doi:10.1016/S0304-4238(03)00106-7
Bukau B, Weissman J, Horwich A (2006) Molecular chaperones and protein quality control. Cell 125:443–451. doi:10.1016/j.cell.2006.04.014
Chen KM, Holmstrom M, Raksajit W, Suorsa M, Piippo M, Aro EM (2010) Small chloroplast-targeted DnaJ proteins are involved in optimization of photosynthetic reactions in *Arabidopsis thaliana*. BMC Plant Biol 10:43. doi:10.1186/1471-2229-10-43
Chen P, Yan K, Shao H, Zhao S (2013) Physiological mechanisms for high salt tolerance in wild soybean (*Glycine soja*) from Yellow River Delta, China: photosynthesis, osmotic regulation, ion flux and antioxidant capacity. PloS ONE 8:e83227. doi:10.1371/journal.pone.0083227
Cyr DM, Lu X, Douglas MG (1992) Regulation of Hsp70 function by a eukaryotic DnaJ homolog. J Biol Chem 267:20927–20931
Dekker SL, Kampinga HH, Bergink S (2015) DNAJs: more than substrate delivery to HSPA. Front Mol Biosci. doi:10.3389/fmolb.2015.00035
DuanMu H et al (2015) Wild soybean roots depend on specific transcription factors and oxidation reduction related genesin response to alkaline stress. Funct Integr Genomics 15:651–660. doi:10.1007/s10142-015-0439-y
Feng CY, Han JX, Han XX, Jiang J (2015) Genome-wide identification, phylogeny, and expression analysis of the SWEET gene family in tomato. Gene 573:261–272. doi:10.1016/j.gene.2015.07.055
Fuglsang AT et al (2007) Arabidopsis Protein Kinase PKS5 Inhibits the Plasma Membrane H^+-ATPase by Preventing Interaction with 14-3-3 Protein. Plant Cell 19:1617–1634 doi:10.1105/tpc.105.035626
Fushimi T, Umeda M, Shimazaki T, Kato A, Toriyama K, Uchimiya H (1994) Nucleotide sequence of a rice cDNA similar to a maize NADP-dependent malic enzyme. Plant Mol Biol 24:965–967
Gong B, Zhang C, Li X, Wen D, Wang S, Shi Q, Wang X (2014) Identification of NaCl and NaHCO3 stress responsive proteins in tomato roots using iTRAQ-based analysis. Biochem Biophys Res Commun 446:417–422. doi:10.1016/j.bbrc.2014.03.005
Guan QJ, Ma HY, Wang ZJ, Wang ZY, Bu QY, Liu SK (2016) A rice LSD1-like-type ZFP gene OsLOL5 enhances saline-alkaline tolerance in transgenic *Arabidopsis thaliana*, yeast and rice Bmc. Genomics 17:142. doi:10.1186/s12864-016-2460-5
Hartl FU, Hayer-Hartl M (2009) Converging concepts of protein folding in vitro and in vivo. Nat Struct Mol Biol 16:574–581. doi:10.1038/nsmb.1591
Hennessy F, Boshoff A, Blatch GL (2005) Rational mutagenesis of a 40 kDa heat shock protein from Agrobacterium tumefaciens identifies amino acid residues critical to its in vivo function. Int J Biochem Cell Biol 37:177–191 doi:10.1016/j.biocel.2004.06.009
Hu B, Jin J, Guo AY, Zhang H, Luo J, Gao G (2015) GSDS 2.0: an upgraded gene feature visualization server. Bioinformatics 31:1296–1297. doi:10.1093/bioinformatics/btu817
Jiang J, Maes EG, Taylor AB, Wang L, Hinck AP, Lafer EM, Sousa R (2007) Structural basis of J cochaperone binding and regulation of Hsp70. Mol Cell 28:422–433. doi:10.1016/j.molcel.2007.08.022
Jose S, Thomas TD (2015) Abiotic stresses increase plant regeneration ability of rhizome explants of *Curcuma caesia* Roxb Plant Cell. Tissue Organ Cult (PCTOC) 122:767–772 doi:10.1007/s11240-015-0795-2
Kampinga HH, Craig EA (2010) The HSP70 chaperone machinery: J proteins as drivers of functional specificity. Nat Rev Mol Cell Bio 11:579–592
Kong F, Deng Y, Wang G, Wang J, Liang X, Meng Q (2014) LeCDJ1, a chloroplast DnaJ protein, facilitates heat tolerance in transgenic tomatoes. J Integr Plant Biol 56:63–74 doi:10.1111/jipb.12119
Kurkela S, Franck M (1990) Cloning and characterization of a cold- and ABA-inducible. *Arabidopsis* Gene Plant Mol Biol 15:137–144
Larkin MA et al (2007) Clustal W and Clustal X version 2.0. Bioinformatics 23:2947–2948. doi:10.1093/bioinformatics/btm404
Lee JA, Woolhouse HW (1969) A comparative study of bicarbonate inhibition of root growth in calcicole and calcifuge grasses. New Phytol 68:1–11 doi:10.1111/j.1469-8137.1969.tb06413.x
Letunic I, Doerks T, Bork P (2015) SMART: recent updates, new developments and status in 2015. Nucleic Acids Res 43:D257–260. doi:10.1093/nar/gku949
Li C, Fang B, Yang C, Shi D, Wang D (2009) Effects of various salt–alkaline mixed stresses on the state of mineral elements in nutrient solutions and the growth of alkali resistant halophyte *Chloris virgata*. J Plant Nutr 32:1137–1147 doi:10.1080/01904160902943163
Li Y, Tan Y, Shao Y, Li M, Ma F (2015) Comprehensive genomic analysis and expression profiling of diacylglycerol kinase gene family in *Malus prunifolia* (Willd.) Borkh. Gene 561:225–234. doi:10.1016/j.gene.2015.02.029
Liu A, Yu Y, Duan X, Sun X, Duanmu H, Zhu Y (2015) GsSKP21, a *Glycine soja* S-phase kinase-associated protein, mediates the regulation of plant alkaline tolerance and ABA sensitivity. Plant Mol Biol 87:111–124 doi:10.1007/s11103-014-0264-z
Munns R (2002) Comparative physiology of salt and water stress. Plant Cell Environ 25:239–250. doi:10.1046/j.0016-8025.2001.00808.x
Nour-Eldin HH, Hansen BG, Norholm MH, Jensen JK, Halkier BA (2006) Advancing uracil-excision based cloning towards an ideal technique for cloning PCR fragments. Nucleic Acids Res 34:e122 doi:10.1093/nar/gkl635
Petti C, Nair M, DeBolt S (2014) The involvement of J-protein AtDjC17 in root development in *Arabidopsis*. Front Plant Sci 5. doi:10.3389/fpls.2014.00532
Piippo M, Allahverdiyeva Y, Paakkarinen V, Suoranta UM, Battchikova N, Aro EM (2006) Chloroplast-mediated regulation of nuclear genes in Arabidopsis thaliana in the absence of light stress. Physiol Genomics 25:142–152. doi:10.1152/physiolgenomics.00256.2005
Pulido P, Toledo-Ortiz G, Phillips MA, Wright LP, Rodriguez-Concepcion M (2013) Arabidopsis J-protein J20 delivers the first enzyme of the plastidial isoprenoid pathway to protein quality control. Plant Cell 25:4183–4194
Qi X et al (2014) Identification of a novel salt tolerance gene in wild soybean by whole-genome sequencing. Nature Commun 5:4340 doi:10.1038/ncomms5340
Qiu XB, Shao YM, Miao S, Wang L (2006) The diversity of the DnaJ/Hsp40 family, the crucial partners for Hsp70 chaperones. Cell Mol Life Sci 63:2560–2570. doi:10.1007/s00018-006-6192-6
Rajan VB, D'Silva P (2009) *Arabidopsis thaliana* J-class heat shock proteins: cellular stress sensors. Funct Integr Genomics 9:433–446 doi:10.1007/s10142-009-0132-0
Rogozin IB, Sverdlov AV, Babenko VN, Koonin EV (2005) Analysis of evolution of exon-intron structure of eukaryotic genes. Brief Bioinform 6:118–134

Salas-Munoz S, Rodriguez-Hernandez AA, Ortega-Amaro MA, Salazar-Badillo FB, Jimenez-Bremont JF (2016) *Arabidopsis* AtDjA3 null mutant shows increased sensitivity to abscisic acid, salt, and osmotic stress in germination and post-germination stages. Front Plant Sci 7:220 doi:10.3389/fpls.2016.00220

Sarkar NK, Thapar U, Kundnani P, Panwar P, Grover A (2013) Functional relevance of J-protein family of rice (*Oryza sativa*). Cell Stress Chaperon 18:321–331

Scarpeci TE, Zanor MI, Carrillo N, Mueller-Roeber B, Valle EM (2008) Generation of superoxide anion in chloroplasts of Arabidopsis thaliana during active photosynthesis: a focus on rapidly induced genes. Plant Mol Biol 66:361–378 doi:10.1007/s11103-007-9274-4

Schultz J, Copley RR, Doerks T, Ponting CP, Bork P (2000) SMART: a web-based tool for the study of genetically mobile domains. Nucleic Acids Res 28:231–234

Seki M, Kamei A, Yamaguchi-Shinozaki K, Shinozaki K (2003) Molecular responses to drought, salinity and frost: common and different paths for plant protection. Curr Opin Biotechnol 14:194–199

Shi D, Wang D (2005) Effects of various salt-alkaline mixed stresses on *Aneurolepidium* chinense (Trin.) Kitag. Plant Soil 271:15–26. doi:10.1007/s11104-004-1307-z

Silver PA, Way JC (1993) Eukaryotic DnaJ homologs and the specificity of Hsp70 activity. Cell 74:5–6

So HA, Chung E, Lee JH (2013) Molecular characterization of soybean GmDjp1 encoding a type III J-protein induced by abiotic stress Genes. Genomics 35:247–256

Steibel J, Poletto R, Rosa G (2005) Statistical analysis of relative quantification of gene expression using real time RT-PCR data. J Dairy Sci 88:104–104

Sun X et al (2015) A 14-3-3 family protein from wild soybean (*Glycine soja*) regulates ABA sensitivity in *Arabidopsis*. PloS ONE 10:e0146163. doi:10.1371/journal.pone.0146163

Sun X et al (2016) A *Glycine soja* methionine sulfoxide reductase B5a interacts with the Ca2+ /CAM-binding kinase GsCBRLK and activates ROS signaling under carbonate alkaline stress. Plant J. doi:10.1111/tpj.13187

Vitha S, Froehlich JE, Koksharova O, Pyke KA, van Erp H, Osteryoung KW (2003) ARC6 is a J-domain plastid division protein and an evolutionary descendant of the cyanobacterial cell division protein Ftn2. Plant Cell 15:1918–1933

Walsh P, Bursac D, Law YC, Cyr D, Lithgow T (2004a) The J-protein family: modulating protein assembly, disassembly and translocation. Embo Rep 5:567–571 doi:10.1038/sj.embor.7400172

Walsh P, Bursac D, Law YC, Cyr D, Lithgow T (2004b) The J-protein family: modulating protein assembly, disassembly and translocation. Embo Rep 5:567–571

Wang H, Datla R, Georges F, Loewen M, Cutler AJ (1995) Promoters from kin1 and cor6.6, two homologous *Arabidopsis thaliana* genes: transcriptional regulation and gene expression induced by low temperature, ABA, osmoticum and dehydration. Plant Mol Biol 28:605–617

Wang ML et al (2004) Gene expression profiles of cold-stored and fresh pollen to investigate pollen germination and growth. Plant Cell physiol 45:1519–1528 doi:10.1093/pcp/pch174

Wang G, Kong F, Zhang S, Meng X, Wang Y, Meng Q (2015) A tomato chloroplast-targeted DnaJ protein protects Rubisco activity under heat stress. J Exp Bot 66:3027–3040. doi:10.1093/jxb/erv102

Wang F, Zhu H, Chen D, Li Z, Peng R, Yao Q (2016) A grape bHLH transcription factor gene, VvbHLH1, increases the accumulation of flavonoids and enhances salt and drought tolerance in transgenic Arabidopsis thaliana Plant Cell. Tissue Organ Cult (PCTOC) 125:387–398 doi:10.1007/s11240-016-0953-1

Weber H, Chetelat A, Reymond P, Farmer EE (2004) Selective and powerful stress gene expression in Arabidopsis in response to malondialdehyde. Plant J 37:877–888

Wu S, Wu M, Dong Q, Jiang H, Cai R, Xiang Y (2015) Genome-wide identification, classification and expression analysis of the PHD-finger protein family in *Populus trichocarpa*. Gene. doi:10.1016/j.gene.2015.08.042

Xu G, Guo C, Shan H, Kong H (2012) Divergence of duplicate genes in exon-intron structure. Proc Natl Acad Sci USA 109:1187–1192. doi:10.1073/pnas.1109047109

Xu W, Jia L, Shi W, Baluska F, Kronzucker HJ, Liang J, Zhang J (2013) The Tomato 14-3-3 Protein TFT4 Modulates H + Efflux, Basipetal Auxin Transport, and the PKS5-J3 Pathway in the Root Growth Response to Alkaline Stress. Plant Physiol 163:1817–1828 doi:10.1104/pp.113.224758

Yang X, Römheld V, Marschner H (1994) Effect of bicarbonate on root growth and accumulation of organic acids in Zn-inefficient and Zn-efficient rice cultivars (*Oryza sativa* L.). Plant Soil 164:1–7. doi:10.1007/bf00010104

Yang C, Chong J, Li C, Kim C, Shi D, Wang D (2007) Osmotic adjustment and ion balance traits of an alkali resistant halophyte Kochia sieversiana during adaptation to salt and alkali conditions. Plant Soil 294:263–276. doi:10.1007/s11104-007-9251-3

Yang Y et al (2010) The *Arabidopsis* chaperone J3 regulates the plasma membrane H^+-ATPase through interaction with the PKS5 kinase. Plant Cell 22:1313–1332. doi:10.1105/tpc.109.069609

Yu Y et al (2016) GsERF6, an ethylene-responsive factor from *Glycine soja*, mediates the regulation of plant bicarbonate tolerance in *Arabidopsis*. Planta. doi:10.1007/s00425-016-2532-4

Zhai Y, Shao S, Sha W, Zhao Y, Zhang J, Ren W, Zhang C (2016) Overexpression of soybean GmERF9 enhances the tolerance to drought and cold in the transgenic tobacco. Plant Cell Tissue Organ Cult (PCTOC) 1–12 doi:10.1007/s11240-016-1137-8

Zhao W, Liu Y-W, Zhou J-M, Zhao S-P, Zhang X-H, Min D-H (2016) Genome-wide analysis of the lectin receptor-like kinase family in foxtail millet (*Setaria italica* L.). Plant Cell Tissue Organ Cult (PCTOC) 127:335–346. doi:10.1007/s11240-016-1053-y